



1 Trends, composition, and sources of carbonaceous aerosol in 2 the last 18 years at the Birkenes Observatory, Northern Europe

3 Karl Espen Yttri¹, Francesco Canonaco^{2,7}, Sabine Eckhardt¹, Nikolaos Evangeliou¹, Markus Fiebig¹,
4 Hans Gundersen¹, Anne-Gunn Hjellbrekke¹, Cathrine Lund Myhre¹, Stephen Matthew Platt¹, André S.
5 H. Prévôt², David Simpson^{3,4}, Sverre Solberg¹, Jason Surratt⁵, Kjetil Tørseth¹, Hilde Uggerud¹, Marit
6 Vadset¹, Xin Wan⁶, and Wenche Aas¹

7
8 ¹NILU - Norwegian Institute for Air Research, P.O. Box 100, N-2027 Kjeller, Norway

9 ²Paul Scherrer Institute (PSI), 5232 Villigen-PSI, Switzerland

10 ³EMEP MSC-W, Norwegian Meteorological Institute, Oslo, Norway

11 ⁴Department of Earth & Space Sciences, Chalmers Univ. Technology, Gothenburg, Sweden

12 ⁵Department of Environmental Sciences & Engineering, University of North Carolina

13 ⁶Key Laboratory of Tibetan Environment Changes and Land Surface Processes, Institute of Tibetan Plateau
14 Research, Chinese Academy of Sciences Courtyard 16, Lin Cui Road, Chaoyang District, Beijing 100101, P.R.
15 China

16 ⁷Datalystica Ltd., 5234 Villigen, Switzerland

17
18 **To whom correspondence should be addressed: Karl Espen Yttri, e-mail address: key@nilu.no*

19 Abstract

20
21 We present 18 years (2001–2018) of aerosol measurements: organic- and elemental carbon (OC and
22 EC), organic tracers (levoglucosan, arabinol, mannitol, trehalose, glucose, 2-methyltetrols), trace
23 elements and ions -at the Birkenes Observatory (Southern Norway), a site representative of the Northern
24 European region. The OC/EC (2001–2018) and the levoglucosan (2008–2018) time series are the longest
25 in Europe, with OC/EC available for the PM₁₀, PM_{2.5} (fine) and PM_{10-2.5} (coarse) size fractions, providing
26 the opportunity for a nearly two-decade long assessment. Using positive matrix factorisation (PMF) we
27 identify six carbonaceous aerosol sources at Birkenes: Mineral dust dominated (MIN), traffic/industry-
28 like (TRA/IND), short range transported biogenic secondary organic aerosol (BSOA_{SRT}), primary
29 biological aerosol particles (PBAP), biomass burning (BB), and ammonium nitrate dominated
30 (NH₄NO₃), and one low carbon fraction, sea salt (SS).

31 We observed significant ($p < 0.05$), large decreases of EC in PM₁₀ ($-3.9\% \text{ yr}^{-1}$) and PM_{2.5} (-4.2%
32 yr^{-1}), and a smaller decline in levoglucosan ($-2.8\% \text{ yr}^{-1}$), suggesting that OC/EC from traffic and industry
33 is decreasing, while abatement of OC/EC from biomass burning has been slightly less successful. EC
34 abatement of anthropogenic sources is further supported by decreasing EC fractions in PM_{2.5} ($-4.0\% \text{ yr}^{-1}$)
35 and PM₁₀ ($-4.7\% \text{ yr}^{-1}$). PMF apportioned 72% of EC to fossil fuel sources, further supported by PMF
36 applied to absorption photometer data, which yielded a two-factor solution with a low aerosol Ångström
37 exponent (AAE=0.93) fraction assumed to be equivalent black carbon from fossil fuel combustion
38 (eBC_{ff}), contributing 78% to eBC mass. The higher AAE fraction (AAE=2.04) is likely eBC from BB



39 (eBC_{bb}). Source receptor model calculations (FLEXPART) showed that Continental Europe and western
40 Russia were the main source regions both of elevated eBC_{bb} and eBC_{fr}.

41 A relative increase in the OC fraction in PM_{2.5} (+3.2% yr⁻¹) and PM₁₀ (+2.3% yr⁻¹) underscores
42 the importance of biogenic sources at Birkenes (BSOA and PBAP), which were higher in the vegetative
43 season and dominated both fine (53%) and coarse (78%) OC. Furthermore, 77–91% of OC in PM_{2.5},
44 PM_{10-2.5} and PM₁₀ was attributed to biogenic sources in summer vs. 22–37% in winter. The coarse
45 fraction had the highest share of biogenic sources regardless of season and was dominated by PBAP,
46 except in winter.

47 Our results show a shift in aerosol composition at Birkenes and thus also in the relative source
48 contributions. The need for diverse off-line and on-line carbonaceous aerosol speciation to understand
49 carbonaceous aerosol sources, including their seasonal, annual, and long-term variability has been
50 demonstrated.

51

52 1. Introduction

53 Carbonaceous aerosol has been studied intensively over the last 20 years due to its influence on
54 radiative forcing (Bond et al., 2013; Myhre and Samset, 2015; Lund et al., 2018), both directly by
55 scattering and absorption of sunlight, and semi directly and indirectly by influencing cloud properties
56 (Boucher et al., 2013; Hodnebrog et al., 2014; Myhre et al., 2013). It also contributes to the burden of
57 respiratory and cardiovascular disease (Janssen et al., 2012; WHO, 2013). Consequently, carbonaceous
58 aerosol [here: elemental carbon (EC) and organic carbon (OC)] is measured regularly in air monitoring
59 networks (e.g., Tørseth and Hov, 2003; Tørseth et al., 2012; UNECE, 2019; Hjellbrekke, 2020).
60 Carbonaceous aerosol has an atmospheric lifetime of days to a few weeks and is thus relevant for
61 atmospheric long-range transport. Accordingly, the European Monitoring and Evaluation Programme
62 (EMEP) included OC/EC measurements in 2004 after a pioneering measurement campaign at 12
63 European sites from 2002–2003 (Yttri et al., 2007a; Tørseth et al., 2012), showing that carbonaceous
64 aerosol was a major constituent of the ambient aerosol in the European rural background environment,
65 accounting for 9–37% (OM = organic matter) and 1–5% (EC) of PM₁₀, and that OM was more abundant
66 than sulfate (SO₄²⁻) at sites reporting both variables (Yttri et al., 2007a). Similar conclusions were found
67 from another long-term campaign, CARBOSOL (Gelencsér et al., 2007; Pio et al., 2007), which
68 monitored atmospheric aerosol and its components for two years at six sites along a west-east transect
69 extending from the Azores, in the mid-Atlantic Ocean, to K-Kusztá (Hungary), in centra Europe.

70 There are numerous carbonaceous aerosol sources, both anthropogenic, e.g. emissions from
71 combustion of fossil fuel and biomass, and biogenic, e.g. vegetation emitted terpene/isoprene oxidation,
72 and primary biological aerosol particles (PBAP) from e.g. plants and fungus (Bauer et al., 2002;
73 Donahue et al., 2009; Hallquist et al., 2009; Fröhlich-Nowoisky et al., 2016).

74 Detailed source apportionment and quantification of carbonaceous aerosol is challenging due to
75 it numerous sources, the complexity of atmospheric formation and the vast number of organic



76 compounds associated with carbonaceous aerosols. A few studies have addressed carbonaceous aerosol
77 sources in the European rural background environment using source-specific organic tracers (Gelencsér
78 et al., 2007; Szidat et al., 2009; Genberg et al., 2011; Gilardoni et al., 2011; Yttri et al., 2011a,b). These
79 consistently show that residential wood burning dominates OC in winter, whereas BSOA is the major
80 source in summer. PBAP makes a significant contribution to PM₁₀ in the vegetative season in the Nordic
81 countries, second only to BSOA (Yttri et al., 2011a,b). Fossil fuel sources typically dominate EC
82 regardless of season but residential wood burning emissions can be equally important and occasionally
83 dominate in the heating season (Zotter et al., 2014; Yttri et al., 2019). On-line high time-resolution
84 measurements by aerosol mass spectrometer (AMS) and aerosol chemical speciation monitors (ACMS)
85 have become available in recent years, complementing off-line analysis of organic tracers. In the
86 comprehensive study by Crippa et al. (2014), including 15 European rural background sites and 2 urban
87 sites, covering winter, spring and fall, hydrocarbon-like organic aerosol (OA) (11±5%) and biomass
88 burning OA (12±5%) contributed almost equally to the total OA concentration. The vast majority was
89 however attributed to secondary sources; i.e., semi volatile oxygenated OA (34±11%) and low-volatility
90 oxygenated OA (50±16%). Secondary oxygenated OA (OOA) can be both anthropogenic and biogenic,
91 however Crippa et al. (2014) did not draw any conclusions on this. Results presented by Bougiatioti et
92 al. (2014) show how freshly emitted biomass burning OA can be transformed to more oxidized OOA
93 after just a short time in the atmosphere when subject to high temperatures and high solar radiation.

94 Over the last decades, European anthropogenic emissions of secondary inorganic aerosol precursors,
95 e.g. ammonia (NH₃) and nitrogen oxides (NO_x), and non-methane volatile organic compounds
96 (NMVOC) have stabilized, and those of sulfur dioxide (SO₂) significantly reduced, following
97 implementation of the Gothenburg Protocol (Reis et al., 2012; UNECE, 2013; Matthews et al., 2020).
98 The anthropogenic carbonaceous aerosol is not regulated by any binding international protocol, although
99 co-benefit is expected from the regulation of NO_x and NMVOC, which act as precursors of secondary
100 organic aerosol (Hallquist et al., 2009). PM_{2.5} was included in the revised version of the Gothenburg
101 protocol (UNECE, 2013) in 2012, which states that effort should be directed towards sources that also
102 emit black carbon (BC), which inevitably also will influence OC.

103 Residential wood burning is a major source of carbonaceous aerosol in circumpolar countries (e.g.
104 Yttri et al., 2014) and even considered the most important source in Norway, accounting for 48% (2017)
105 of PM_{2.5} (Grythe et al., 2019). This region also regularly experiences major wild and agricultural fires
106 (e.g. Stohl et al., 2006 and 2007). A growing number of studies show that residential wood burning is
107 more widespread in continental Europe than previously assumed and that its contribution to the ambient
108 carbonaceous aerosol can be substantial (Sillanpää et al., 2006; Gelencsér et al., 2007; Puxbaum et al.,
109 2007; Lanz et al., 2010; Maenhaut et al., 2012; Genberg et al., 2013; Fuller et al., 2014; Yttri et al.,
110 2019) and even dominating (Szidat et al., 2007; Herich et al., 2014). Residential wood burning is a
111 decentralized source in Europe and combustion typically takes place in small units where the emissions
112 are emitted without after-treatment. An economic downturn in Greece compelled households to burn



113 firewood and waste material as fuel costs rose, increasing residential wood burning emissions in urban
114 areas by 30% (Saffari et al., 2013). Future increases in European wood burning emissions might occur
115 due to climate change mitigation policies supporting the use of renewable and biofuels (van der Gon et
116 al., 2015). Denier van der Gon et al. (2015) conclude that European emissions from residential wood
117 burning are significantly underestimated, thus it appears timely to address how ambient carbonaceous
118 aerosol -particularly from biomass burning -have developed over the last two decades.

119 Kahnert et al. (2004) and Tørseth et al. (2012) highlight the importance of long-term measurements
120 (> 10 years) of carbonaceous aerosol. The Birkenes Observatory in southern Norway holds the longest
121 time series of OC and EC in Europe, dating back to 2001, including measurements in both the PM₁₀ and
122 the PM_{2.5} fractions. Downwind of major anthropogenic emission regions in Europe, the Birkenes
123 Observatory is well suited to monitor air pollution from Continental Europe.

124 Here we apply positive matrix factorization (PMF) to identify sources of carbonaceous aerosol at
125 the Birkenes Observatory. Measurements of complementary species accompany OC/EC monitoring,
126 allowing us to understand these sources, their contribution and variability at time scales from minutes
127 to decades: organic tracers for biomass burning (levoglucosan), PBAP (arabitol, mannitol, trehalose and
128 glucose) and BSOA (2-methyltetrols), as well as high time resolution equivalent black carbon resulting
129 from biomass (eBC_{bb}) and fossil (eBC_{ff}) fuel combustion, derived from multiwavelength aethalometer
130 measurements.

131

132 2. Methodology

133 2.1 Sampling site

134 The Birkenes Observatory (58°23'N, 8°15'E, 219 m above sea level, asl) is an EMEP/GAW (Global
135 Atmospheric Watch) supersite in southern Norway (Figure 1). The observatory is in the Boreo-nemorale
136 zone with mixed coniferous and deciduous trees (65% of the land use near the site); the remainder being
137 meadows (10%), low intensity agricultural areas (10%), and freshwater lakes (15%). Close to the
138 Skagerrak coast (~20 km) and at low altitude, the observatory experiences a maritime climate with
139 relatively mild winters and moderately warm summers. The prevailing wind is westerly/south westerly.
140 Figure S 1 shows ambient temperature and precipitation (2001–2018) at Birkenes. The nearest city is
141 Kristiansand (population ~61 000) 25 km to the south/south-west.

142

143 2.2 Measurements and procedures

144 2.2.1 Off-line filter measurements

145 We collected OC/EC, organic tracers and PM mass filter samples using two low-volume samplers with
146 a PM₁₀ and a PM_{2.5} inlet. Quartz fiber filters (Whatman QM-A; 47 mm in diameter) were pre-fired (850
147 °C; 3 h). We conditioned the filters [20 ± 1 °C; 50 ± 5% RH (relative humidity)] for 48 h before and after
148 exposure and weighed them to obtain PM mass. We kept filters in petri slides and stored them at 4 °C
149 after weighing and before OC/EC analysis. After OC/EC analysis and prior to organic tracer analysis



150 the samples were stored at $-18\text{ }^{\circ}\text{C}$. Two field blanks were assigned to each month of sampling and were
151 treated in exactly the same manner regarding preparation, handling, transport and storage as the exposed
152 filters, except that they were not inserted in the samplers. We collected one sample per sampler per week
153 (168 hours), except for 14 August 2002–17 September 2008, when two samples were collected per
154 sampler per week; at 24 h and 144 h intervals. The sampling inlets are 2 m above the Observatory roof,
155 5 m above the ground level ($\sim 226\text{ m asl}$). The OC/EC and PM mass time series date back to February
156 2001 and organic tracers back to January 2008 (monosaccharide anhydrides) and January 2016 (sugars,
157 sugar-alcohols and 2-methyltetrols).

158 We performed thermal-optical analysis (TOA, Sunset Laboratory OC/EC instrument), using
159 transmission for charring correction. We used the Quartz temperature programme in 2001–2008 and
160 EUSAAR-2 (Cavalli et al., 2010) from 2008. We compare the two temperature programmes for $\text{PM}_{2.5}$
161 samples collected in 2014 in Supplementary Sect. S1. OC/EC instrument performance is regularly inter-
162 compared under the joint EMEP/ACTRIS quality assurance and quality control effort (e.g. Cavalli et
163 al., 2013).

164 Until 2014, we determined monosaccharide anhydrides (levoglucosan, mannosan, galactosan)
165 in PM_{10} using high-performance liquid chromatography high-resolution time-of-flight mass
166 spectrometry (HPLC-HR-TOFMS) in negative electrospray ionization mode according to the method
167 of Dye and Yttri (2005). After 2014, we use ultra-performance liquid chromatography (UPLC), with
168 two Waters columns ($2 \times 2.1 \times 150\text{ mm HSS T3}$, $1.8\text{ }\mu\text{m}$, Waters Inc.). Changing the column improved
169 the chromatographic resolution, allowing the analysis of sugars, sugar-alcohols and 2-methyltetrols. We
170 identified the monosaccharides anhydrides based on retention time and mass spectra (accurate mass and
171 isotope pattern) of authentic standards (Table S 1). Isotope-labelled standards of levoglucosan,
172 galactosan, arabitol, mannitol, trehalose and glucose were used as internal recovery standard (Table S
173 1).

174 Weekly OC/EC, PM_{10} , $\text{PM}_{2.5}$ are publicly available on EBAS (<http://ebas.nilu.no>). Mean values
175 (daily/weekly/seasonal/annual) used below, merging of data from the old and new Birkenes sites, and
176 quality assurance of the filter data are detailed in Sect. S1. We used the Mann-Kendall test (Mann, 1945;
177 Kendall, 1975; Gilbert, 1987) to identify significant trends in the filter based measurements, and the
178 Theil-Sen slope (Theil, 1958; Sen, 1968; Gilbert, 1987) to quantify the trends (Sect. S2).

179

180 2.2.2 Online measurement and source apportionment of absorption coefficients

181 We determined Absorption coefficients (B_{Abs}) using a multi-wavelength absorption photometer (AE33
182 Aethalometer, Magee Scientific. Here we performed source apportionment using the aethalometer
183 model (Sandradewi et al., 2008) to determine $\text{eBC}_{\text{bb}}/\text{eBC}_{\text{fr}}$. However, the aethalometer model requires
184 *a-priori* knowledge of the aerosol Ångström exponents (AAE), uncertainties in which can lead to large
185 variation in the magnitude of the resulting time series and negative concentrations during some periods.
186 Often, the aethalometer model yields negative concentrations for any single input AAE pair. Therefore,



187 we also used a novel positive matrix factorization (PMF) application finding two factors, a low AAE
188 factor (0.9) and a higher AAE factor (2.04) identified as eBC_{fr} and eBC_{bb}, respectively. Uncertainties
189 were assessed using bootstrapping ($n=2000$). The advantages of the PMF are that no *a-priori* knowledge
190 of the factor AAEs is required, no periods of negative concentration result, deviations from a strict
191 power-law dependence of B_{Abs} on wavelength (e.g. due to degradation of light absorbing components in
192 the atmosphere or instrument errors/bias) are permitted, and poorly fitting data are assigned to a residual.
193 Meanwhile bootstrapping allows estimation of uncertainties, the methodology of the PMF analysis and
194 aethalometer data post-processing are detailed in Sect. S3 (Table S 2).

195

196 **2.3 FLEXPART model simulations**

197 We investigated the origin of the observed eBC with a Lagrangian transport model (FLEXPART v10.4,
198 Pisso et al., 2019). The model, powered by European Centre for Medium-Range Weather Forecasts with
199 137 vertical layers and a horizontal resolution of $0.1^\circ \times 0.1^\circ$ tracks simulated particles arriving at the
200 receptor 30 days backwards in time (retro-plume mode) and accounts for gravitational settling, dry and
201 wet deposition (Grythe et al., 2017), turbulence (Cassiani et al., 2014), unresolved mesoscale motions
202 (Stohl et al., 2005) and includes a deep convection scheme (Forster et al., 2007). Output consists of an
203 emission sensitivity ($0.5^\circ \times 0.5^\circ$ resolution), a quantitative measure for the particle mass concentration at
204 the receptor resulting from a unit emission flux at the Earth's surface. The emission sensitivity can also
205 be interpreted as a probability distribution field of the particle's origin, used in the present study to
206 identify possible source regions of eBC.

207

208 **2.4 Positive Matrix Factorisation analysis on filter data**

209 We performed PMF (See Sect. S3 for a description of the analysis principal and S4 for its application to
210 filter data) using the following as input data: OC (in PM_{2.5} and PM_{10-2.5}), EC (in PM₁₀), levoglucosan,
211 mannosan, galactosan, arabitol, mannitol, trehalose, glucose, V, Mn, Ti, Fe, Co, Ni, Cu, Zn, As, Cd, and
212 Pb (all in PM₁₀), SO₄²⁻, NO₃⁻, NH₄⁺, Ca²⁺, Mg²⁺, K⁺, Na⁺, Cl⁻ (from open filter face). Table S 3 shows
213 miscellaneous settings of the PMF analysis of these data including missing data treatment and an
214 assessment of the PMF performance. The input data and error estimates were prepared using the
215 procedure suggested by Polissar et al. (1998) and Norris et al. (2014), see Sect. S3.

216 Source apportionment via PMF is based on the temporal variability of the components. It is
217 expected that significant contributions to carbonaceous aerosol at Birkenes is via long-range
218 atmospheric transport (LRT), alongside more local sources. Local and LRT sources will have different
219 temporal variability, and significant mixing of air masses and chemical transformation is expected for
220 the latter, i.e., factor profiles at Birkenes are expected to differ somewhat from emission profiles at the
221 source, even though the profile is distinctive enough for source attribution. Because of this we did not
222 attempt to constrain factor profiles via e.g. ME-2 (Canonaco et al., 2013) since Birkenes, as a relatively
223 clean rural background site, is unlikely to receive unprocessed emissions. Furthermore, mixed



224 contributions to a factor can in some cases be resolved *a posteriori* for source quantification (i.e. if it is
225 clear where mass should be reassigned), without potentially perturbing the output factor time series.

226

227 **2.4.1 Identification of PMF factors**

228 The BB factor appears well confined in the PMF solution (Figure 2, Table S 4), explaining all the
229 monosaccharide anhydrides (95–98%). OC_{BB} was almost exclusively (87%) in the fine fraction of PM₁₀.
230 Other key qualifiers derived from the BB factor are the ratios listed in Table 1, which are highly
231 comparable to the results obtained by ¹⁴C-analysis reported in the comprehensive study by Zotter et al.
232 (2014). The BB factor is elevated in the heating season and peaks in winter, pointing to residential
233 heating as the major source.

234 The TRA/IND factor explained most EC (50%), the majority of the trace elements Pb (84%),
235 Zn (82%), Cd (81%), As (78%), V (70%), Ni (69%), Cu (62%) and Co (42%) and a noticeable fraction
236 of SO₄²⁻ (20%), which suggests influence of various anthropogenic emissions. IND/TRA explained a
237 small fraction of fine OC (10%) and a negligible fraction of coarse OC (4%). The majority of OC (88%)
238 resides in the fine fraction, which is in line with its combustion-derived origin. The high EC fraction
239 unambiguously points to combustion processes, and the low OC/EC ratio (1.4 for PM_{2.5}) towards a
240 substantial, but not exclusive, influence from vehicular traffic. Cu and Zn result from brake wear (Fomba
241 et al., 2018), whereas tire wear is an additional source of Zn (Pacyna et al., 1996), corroborating the
242 influence of vehicular traffic to the TRA/IND factor. Ni and V are commonly associated with
243 combustion of heavy oil (Viana et al., 2008), As, Cd and Pb with combustion of coal, and to a lesser
244 extent oil, but also from metallurgic activity (Pacyna et al., 1986). The TRA/IND factor has a minimum
245 in summer and shows minor variability for the rest of the year. A similar drop in the vehicular traffic
246 factor in summer for Helsinki was shown by Saarikoski et al. (2008).

247 The PMF analysis confined the majority of coarse OC (53%) and essentially all (82–93%) of
248 the PBAP tracers (arabitol, mannitol, trehalose, and glucose) within one factor (PBAP). The PBAP
249 factor has a pronounced seasonal variability with increased levels in the vegetative season and nearly
250 absent outside of it, as previously described for coarse OC (Yttri et al., 2007a) and PBAP tracers (Yttri
251 et al., 2007b) at Birkenes.

252 2-methyltetrols (92–96%) are oxidation products of isoprene (Claeys et al., 2004) and are almost
253 exclusively attributed to the BSOA_{SRT} (SRT=Short Range Transport) factor, which explains 9% of fine
254 OC and 13% of coarse OC. The complete absence of EC and the presence of SO₄²⁻ (17%) underpins the
255 secondary nature of this factor, which is present in summer with tail ends in late spring an early fall. The
256 BSOA_{SRT} time series increases abruptly in the transition May/June, as leaves unfold, and subsides
257 equally rapid in the beginning of October when trees shed their leaves. The near absence of 2-
258 methyltetrols prior to May/June suggests that the 0.5–1.5 months earlier onset of the vegetative season
259 in Continental Europe (Rötzer and Chmielewski, 2001) is not reflected by the 2-methyltetrols
260 observations at Birkenes, indicating a short atmospheric lifetime for 2-methyltetrols. Consequently,



261 local isoprene emissions likely explain the observed concentrations of 2-methyltetrols at Birkenes,
262 questioning to what extent the $BSOA_{SRT}$ factor includes a continental BSOA contribution. Similar
263 sources (deciduous and coniferous trees), temperature dependent emissions, and formation rates, suggest
264 that particulate phase oxidation products of mono- and sesquiterpenes are accounted for by the isoprene-
265 derived $BSOA_{SRT}$ -factor as well, but with a similar issue concerning local versus LRT contribution, as
266 proposed for the 2-methyltetrols.

267 The MIN factor is defined by its content of Ti (93% of total), Fe (75%), Mn (52%) and Ca^{2+}
268 (39%) (Figure 2, Table S 4), well-known constituents of mineral dust (e.g. Alastuey et al., 2016). It also
269 contains some of the elements that dominate the TRA/IND factor, including Co (43%), Cu (20%), Ni
270 (17%) and V (14%), indicating anthropogenic influence. Notably, 31% of fine OC is attributed to the
271 MIN factor, whereas it explains 13% of coarse OC. This corresponds to that reported by Kyllönen et al.
272 (2020) for the Subarctic site Pallas (Finland) where 29% of the fine OC was apportioned to the mineral
273 dust factor. Waked et al. (2014) found a similar result for Lens (France) where the mineral dust factor
274 explained 15% of OC. No information on the size distribution was available in Kyllönen et al. (2020)
275 and Waked et al. (2014), whereas in the present study 86% of OC in the MIN factor resides in the fine
276 fraction of PM_{10} . Since mineral dust typically resides in the coarse fraction of PM_{10} (Ripoll et al., 2015),
277 one would expect the same for its carbon content, e.g. as $CaCO_3$. More efficient deposition of coarse
278 mode mineral dust during LRT is one possible explanation but mixing of air masses is more likely, as
279 13% of the EC also resides in this factor. The high OC/EC ratio in the unweighted MIN factor profile
280 (18 for $PM_{2.5}$) indicates a minor primary combustion particle influence, and the absence of levoglucosan
281 shows that the EC content originates from fossil fuel combustion (consistent with some TRA/IND
282 influence). Using Eq. (1), 8% of the MIN factor's fine OC content is attributed to combustion of fossil
283 fuel OC (OC_{PrimFF}), whereas the corresponding percentage for PM_{10} OC is 7%. If all Ca^{2+} and Mg^{2+} in
284 the MIN factor was present as either Calcite ($CaCO_3$) or Dolomite $CaMg(CO_3)_2$, the CO_3^{2-} -carbon would
285 account for no more than 3% of the factor's PM_{10} OC content, and 22% if all reside in its coarse fraction.
286 This shows that the OC content of the MIN factor mostly originates from other sources than mineral
287 dust and combustion of fossil fuel. The MIN factor is most abundant in spring and early summer, as
288 seen by Waked et al. (2014), and is associated with southern air masses, as seen for the dry and warm
289 period in the transition of May/June 2018 (Figure 3) when there was a pronounced peak in the MIN
290 factor time series (Figure 2). Indeed, the mean ambient temperature was 4°C higher in May 2018 than
291 for May 2001–2018, whereas it was 2.4°C higher for June 2018 than for June 2001–2018. We thus
292 suggest that the climatological conditions that activate mineral dust sources also favours BSOA
293 formation and that the majority of both fine (92%) and coarse fraction (78%) OC in the MIN factor is
294 LRT BSOA ($OC_{BSOA,LRT}$).

295

$$296 \quad OC_{Fossil,primary,MIN} = [EC_{MIN}] \times \left(\frac{OC}{EC}\right)_{TRA/IND}, \left(\frac{OC}{EC}\right)_{TRA/IND} = 1.4 \quad Eq. 1$$

297



298 The majority of NH_4^+ (77%) and NO_3^- (68%) reside in the NH_4NO_3 factor, which points to
299 secondary inorganic aerosol (SIA) formation during LRT. This is supported by a noticeable contribution
300 of SO_4^{2-} (35%) to the NH_4NO_3 factor, as well. The factors content of NO_2 (30%) points towards a
301 combustion-derived origin of NO_3 , as does EC (13%). The factor's OC content is comparable to that
302 seen for the BB factor. The factor is most pronounced in winter and spring.

303 The SS factor was recognized by its high Cl^- (96%), Na^+ (87%) and Mg^{2+} (79%) fractions. The
304 K^+/Na^+ (0.036), $\text{Ca}^{2+}/\text{Na}^+$ (0.034) and $\text{SO}_4^{2-}/\text{Na}^+$ (0.282) ratios derived from the SS factor closely
305 resembles these ratios in sea water (0.037, 0.038 and 0.252) (Stumm and Morgan, 1995), further
306 demonstrating the successful separation of this factor.

307

308 3. Results and discussion

309 3.1 Levels and trends of carbonaceous aerosol and organic tracers

310 Annual mean carbonaceous aerosol concentrations at Birkenes (2001–2018) are among the lowest in
311 Europe (Yttri et al., 2007a; Yttri et al., 2019), with OC from 0.56–1.07 $\mu\text{g C m}^{-3}$ for PM_{10} and 0.50–
312 0.93 $\mu\text{g C m}^{-3}$ for $\text{PM}_{2.5}$, and EC from 0.05–0.15 $\mu\text{g C m}^{-3}$ (Figure 4; Table S 4). EC, being from
313 combustion that generates fine PM, was almost exclusively associated with $\text{PM}_{2.5}$, whereas OC was
314 abundant also in the coarse fraction ($\text{PM}_{10-2.5}$), particularly in summer and fall (Figure 4). The
315 correlation between OC and EC varied by season (Table S 6) and was highest in the heating season,
316 reflecting the contribution of biogenic, non-EC sources, such as BSOA and PBAP in the vegetative
317 season. The higher R^2 -values for $\text{PM}_{2.5}$ compared to PM_{10} can partly be attributed to PBAP, which
318 mainly resides in $\text{PM}_{10-2.5}$.

319 The variability of the annual mean OC (15–22%) and EC (27%) concentrations was comparable
320 to the major secondary inorganic aerosol (SIA) (SO_4^{2-} , NO_3^- , NH_4^+) and sea salt (SS) aerosol species
321 (Na^+ , Mg^{2+} , Cl^-) (25–31%). A difference of > 60% between consecutive years was observed for OC and
322 EC in PM_{10} and $\text{PM}_{2.5}$, whereas 160% was seen for OC in $\text{PM}_{10-2.5}$. It is important to note that despite
323 decades of SO_2 , NH_3 and NO_x mitigation efforts, SIA dominates PM_{10} mass (29–52%) most years,
324 followed by carbonaceous aerosol (24–40%) and SS aerosol (10–28%) (Figure 5; Table S 7). SIA
325 constituents were also the largest PM_{10} fraction during air pollution episodes (Table S 8), reflecting that
326 Birkenes is affected by major SIA precursor emission regions in Continental Europe.

327 Levels of total carbon (TC) and PM fractions are shown in Table S 9 and Table S 10, respectively
328 for completeness. In the following sections we discuss the OC and EC fractions separately in detail.

329

330 3.1.1 Organic carbon

331 We found no significant trend for OC in PM_{10} ($\text{OC}_{\text{PM}_{10}}$). For fine OC in $\text{PM}_{2.5}$ ($\text{OC}_{\text{PM}_{2.5}}$) there was a
332 minor decrease ($-0.8\% \text{ yr}^{-1}$), whereas there was a minor increase for coarse OC ($\text{OC}_{\text{PM}_{10-2.5}}$) ($0.8\% \text{ yr}^{-1}$)
333 (Table S 11). The anthropogenic fraction of OC observed at Birkenes likely has a downward trend as
334 found for EC, (Sect. 3.1.2) but the substantial influence of natural sources demonstrated in the present,



335 as well as in previous, studies (Yttri et al., 2011b), explains the general lack of trends for OC.
336 The OC time series are characterized by two years where the annual mean was substantially
337 higher (2006) and lower (2012) than the proceeding and the following year (Figure 4). The increased
338 level in 2006 was most pronounced in the fine fraction and in all seasons except spring, whereas the
339 drop in 2012 mainly was attributed to the coarse fraction and was observed in all seasons. The $OC_{PM_{10-2.5}}$
340 annual mean time series is characterised by a stepwise increase from 2001 up to, and including, 2006,
341 after which the concentration dropped and showed minor annual variability, except for the very low
342 annual mean of 2012. After 2015, there are indications of a similar stepwise increase as seen for 2001–
343 2006.

344 The $OC_{PM_{10-2.5}}$ contribution to $OC_{PM_{10}}$ ranged from 18–35% on an annual basis (2001 excluded due to
345 data capture <50%), and levels were highest in summer and fall. Previous studies (Simpson et al.,
346 2007; Yttri et al., 2011a,b) showed that BSOA largely dominates the fine carbonaceous aerosol in
347 summer at Birkenes, whereas the present study shows that Birkenes regularly experiences major air
348 pollution events in spring, as a result of long-range atmospheric transport (LRT) (Table S 4, Table S 7
349 and Table S 8. Hence, both biogenic sources and LRT explain the observed seasonality of fine OC.

350 We attribute elevated $OC_{PM_{2.5}}$ in winter 2010 to residential wood burning emissions as discussed
351 in Sect. 3.2.1. Only on five occasions did the seasonal mean of $OC_{PM_{2.5}}$ exceed $1 \mu\text{g C m}^{-3}$, four of those
352 in the first three years of the time series. The highest mean was observed in summer 2002 ($1.4 \mu\text{g C m}^{-3}$)
353 when wildfires in Eastern Europe influenced Birkenes (Yttri et al., 2007a). The four other occasions,
354 spring (2001, 2002, 2003 and 2018), also saw prolonged episodes of PM air pollution with the hallmark
355 of LRT; i.e., elevated SO_4^{2-} , NO_3^- and NH_4^+ . According to our PMF analysis (See Sect. 3.2) there are
356 several anthropogenic and biogenic sources likely to contribute to fine OC at Birkenes, whereas coarse
357 fraction OC is dominated by a single source, PBAP (Yttri et al., 2007 a,b; Yttri et al., 2011 a,b; Glasius
358 et al., 2018). Hence, it is not surprising that $OC_{PM_{2.5}}$ was the dominant OC fraction, accounting for 70–
359 89% $OC_{PM_{10}}$ on an annual basis.

360

361 3.1.2 Elemental carbon

362 Notably, EC levels dropped from 2007–2008, contrasting with the annual mean OC time series,
363 (Figure 4 and Table S 4). This major downward trend of EC clearly points to changing source
364 contributions to EC at Birkenes. We rarely observed seasonal means exceeding $0.15 \mu\text{g C m}^{-3}$; only in
365 winter 2006, 2007 and 2010, spring 2001, 2003 and 2007, and fall 2005 and 2011. Weekly samples
366 exceeded $0.5 \mu\text{g C m}^{-3}$ for three samples only, all associated with LRT.

367 A statistically significant reduction was calculated for EC in PM_{10} ($-3.9\% \text{ yr}^{-1}$) and $PM_{2.5}$ (-4.2%
368 yr^{-1}) (Table S 11), corresponding well with SO_4^{2-} ($-3.8\% \text{ yr}^{-1}$) and $PM_{2.5}$ ($-4.0\% \text{ yr}^{-1}$). The trend for EC
369 was most pronounced in spring and summer ($-4.0 - -5.9\% \text{ yr}^{-1}$) (Table S 12), as seen for SO_4^{2-} ($-4.2 - -$
370 $6.4\% \text{ yr}^{-1}$) and $PM_{2.5}$ ($-3.0 - -4.4\% \text{ yr}^{-1}$) (Table S 12). The EMEP model finds a somewhat lower
371 reduction for EC ($-3.0\% \text{ yr}^{-1}$) for 2001–2017 (EEA, 2020) with the largest emission reductions for the



372 road transport (83 kt; $-3.6\% \text{ yr}^{-1}$) and off-road categories (44 kt; $-3.7\% \text{ yr}^{-1}$) (<https://www.ceip.at>), which
373 are sectors with a minor seasonal variability. We suggest that these sectors explain the downward trend
374 observed for EC at Birkenes, and that the seasonality of the EC trend is due to the substantial contribution
375 from less abated sources, such as domestic heating in winter and fall. Notably, modelled EC emissions
376 are unchanged for the category other stationary combustion for 2001–2016 (-1 kt ; $-0.08\% \text{ yr}^{-1}$)
377 (<https://www.ceip.at>), which includes residential heating, and wood burning in particular.

378 Effective abatement of SIA precursors and fossil EC, along with a high natural source
379 contribution to OC, largely explains why the OC fraction increased significantly for $\text{PM}_{2.5}$ ($+3.2\% \text{ yr}^{-1}$)
380 and PM_{10} ($+2.4\% \text{ yr}^{-1}$), whereas it decreased for the EC fraction ($-3.9 - -4.5\% \text{ yr}^{-1}$) (Table S 13). The
381 largest increase (OC) and decrease (EC) was seen in the vegetative season (Table S 14) when BSOA
382 and PBAP increase and the influence of poorly abated sources such as domestic heating is low.
383 Consequently, these results demonstrate a long-term change in the aerosol chemical composition at
384 Birkenes and thus also in the relative source composition of PM.

385

386 3.1.3 Levoglucosan

387 Levels of levoglucosan and other organic tracers are given in Table S 15, whereas other organic tracers
388 (arabitol, mannitol, trehalose, glucose, and 2-methyltetrols) are discussed in Sect. S6.

389 The statistically significant decrease of levoglucosan ($-2.8\% \text{ yr}^{-1}$) at Birkenes for 2008–2018
390 (Figure 6; Table S 11), and the fact that biomass burning levels observed at Birkenes are largely
391 explained by continental emissions (Figure 7) might indicate that wood burning emissions in continental
392 Europe are declining. However, surprisingly, we find no significant trend for levoglucosan on a seasonal
393 basis (Table S 12). Furthermore, and although one should be careful drawing conclusions from non-
394 significant outcomes, it is worth noting that the levoglucosan to EC ratio most likely increased ($+2.8\%$
395 yr^{-1} , $\text{CI} = -3.5 - +6.5\% \text{ yr}^{-1}$ and $+2.3\% \text{ yr}^{-1}$, $\text{CI} = -2.2 - 5.0\% \text{ yr}^{-1}$) for the period 2008–2018, whereas it
396 most likely decreased (-1.8 , $\text{CI} = -10.6 - +1.8$ and $-3.6\% \text{ yr}^{-1}$, $\text{CI} = -9.8 - +1.3\% \text{ yr}^{-1}$) for the levoglucosan
397 to OC ratio (Table S 13). A more efficient abatement of fossil sources than biomass burning would
398 explain the levoglucosan to EC increase, whereas we fail to see a similar trend for the levoglucosan to
399 OC ratio, as prevailing natural sources mask the assumed reduction in fossil OC of anthropogenic origin.

400 The levoglucosan time-series provides a hitherto unprecedented opportunity to validate European
401 residential wood burning emission inventories at a decadal time basis. Unfortunately, the inventories
402 suffer from non-harmonized emission reporting and lack of condensable organics (van der Gon et al.,
403 2015, Simpson et al., 2019), which hampers any reliable attempt for such validation. Given the
404 uncertainties in the trend calculations (i.e. annual vs. seasonal trends), more work is needed to
405 investigate trends in levoglucosan and biomass burning, foremost by continuation of the actual time
406 series. Such efforts should be initiated immediately given the numerous studies that point to residential
407 wood burning as a major source of air pollution in Europe (e.g. Denier van der Gon et al., 2015; Yttri
408 et al., 2019).



409

410 3.2 Sources of carbonaceous aerosol at Birkenes

411 We used PMF to apportion carbonaceous aerosol at Birkenes for 2016–2018. The time period was
412 restricted by organic tracer data availability. Carbonaceous aerosol annual means for 2016–2018 were
413 within the long-term annual mean (\pm SD) for OC, and only slightly lower for EC in 2016 and 2017 and
414 are thus representative of the longer time series. Six out of seven factors identified in contribution-
415 weighted relative profiles from PMF (Figure 2; Table S 4) were associated with significant amounts of
416 carbonaceous aerosol. This includes factors for mineral dust-dominated (MIN), which OC content is
417 associated mainly with LRT BSOA ($BSOA_{LRT}$), traffic/industrial-like (TRA/IND), biogenic secondary
418 organic aerosol ($BSOA_{SRT}$), which is short-range transported, primary biological aerosol particles
419 (PBAP), biomass burning (BB), and ammonium nitrate dominated (NH_4NO_3). The sea salt aerosol factor
420 (SS) had a negligible ($<1\%$) carbonaceous aerosol content.

421 The MIN factor (31%) explained the largest fraction of fine OC, whereas BB (17%), NH_4NO_3
422 (17%) and PBAP (16%) had almost equally large shares, as did IND/TRA (10%) and $BSOA_{SRT}$ (9%)
423 (Figure 8). Coarse OC was by far most abundant in the PBAP factor (53%), whereas $BSOA_{SRT}$ (13%),
424 MIN (13%) and NH_4NO_3 (12%) explained almost equally large shares. For the other factors, coarse OC
425 was minor. EC was apportioned to only five factors of which TRA/IND (50%) dominated by far. BB
426 made a 21% contribution and MIN and NH_4NO_3 equally large shares (13%). The 3% apportioned to
427 PBAP is an assumed analytical artefact (See Sect. 3.2.2 for details).

428 The BB, NH_4NO_3 and TRA/IND factors are considered entirely anthropogenic, $BSOA_{SRT}$ and
429 PBAP exclusively natural, whereas MIN is mixed (Figure 8). Natural (54%) and anthropogenic (46%)
430 sources contributed almost equally to fine OC (Figure 8) annually, so also in spring and fall (51%
431 natural), whereas natural sources prevailed in summer (77%) and anthropogenic in winter (78%).
432 Natural sources dominated coarse OC annually (78%) and in all seasons (70–91%), except winter (37%).
433 We consider the minor fraction of coarse OC attributed to carbonate-carbon (3%) to be of natural origin.
434 The findings for OC in PM_{10} are rather like that of $PM_{2.5}$, only that the natural contribution is somewhat
435 more pronounced due to the influence from a mostly naturally influenced coarse OC fraction.

436

437 3.2.1 Anthropogenic carbonaceous aerosol sources

438 According to PMF, BB accounted for 14–17% of OC annually, considering both $PM_{2.5}$ and PM_{10} vs.
439 only 6% of coarse OC. BB was by far the major contributor to OC in winter (35–37%) and by far the
440 most minor contributor in summer (2–3%) (not considering SS). Spring and fall are transition seasons
441 where BB still made a substantial 14–19% contribution to OC. BB explained 22% of EC annually
442 (excluding EC_{PBAP} , which we assume is an analytical artefact, see Sect. 3.2.2), hence fossil fuel
443 combustion (78%) was the major source. Emissions from residential wood burning increased in the
444 heating season but fossil fuel sources dominated EC even in winter (66%). It cannot be excluded that
445 part of levoglucosan originates from wildfires in summer, spring, and fall, though this itself may be due



446 to anthropogenic activity. However, the levoglucosan/mannosan (L/M) ratio indicates minor variability
447 in the source composition throughout the year (See Sect. S5), suggesting one dominating source.
448 The 78%:22% split of EC into fossil fuel combustion and biomass burning derived from PMF is
449 supported by high time resolved concentrations of eBC_{BB} and eBC_{FF} derived from multiwavelength
450 aethalometer measurements of the absorption coefficient, following the PMF-approach of Platt et al.
451 (in prep.). With this approach we find $eBC_{BB}/eBC_{TOT}=28\%$ (Table 2). Meanwhile, using the
452 aethalometer model and $AAE_{FF}=0.9$ and $AAE_{BB}=1.68$ (Zotter et al. 2017) as input we find
453 $eBC_{BB}/eBC_{TOT}=48\%$, however the aethalometer model is extremely sensitive to the input AAE and the
454 AAE values suggested by Zotter et al. (2017) are only recommended where no *a priori* information on
455 the AAEs is available and a significant advantage of the PMF approach by Platt et al., (in prep.) is that
456 the AAE is an output.

457 Source regions of elevated (70th percentile) and low (30th) winter and summertime eBC_{BB} (and
458 eBC_{FF}) observed at Birkenes for 2018 were studied using the approach of Hirdman et al. (2010). The
459 results show that Birkenes is a receptor of LRT exclusively from Continental Europe for elevated eBC_{BB}
460 and eBC_{FF} levels (Figure 7), both in summer and winter. This is consistent with a lack of diurnal
461 variation in either eBC_{BB} or eBC_{FF} , likely because there are few local sources at Birkenes. The main
462 source regions extend from the Atlantic coast in the west to the Ural Mountains in winter, whereas the
463 regions in summer are confined to Eastern Europe and western Russia (but not as far east as the Urals).
464 Notably, the Nordic countries do not contribute to elevated levels except for southern parts of Finland
465 in summer. The footprints are almost identical for eBC_{BB} and eBC_{FF} both for summer and winter. High
466 similarity in winter is not a surprise, as the footprint covers such a wide area and because wood burning
467 for residential heating is common in several European countries. The summertime footprint is a
468 subsection of the wintertime footprint that covers an area well-known for severe wildfires and
469 agricultural fires (Stohl et al., 2007 and Yttri et al., 2007a), and thus agrees with previous studies.
470 Further, Sciare et al. (2008) point to the European countries bordering the Black Sea as having high
471 carbonaceous aerosol of fossil origin. Low eBC_{BB} and eBC_{FF} levels at Birkenes are consistent with
472 air masses that have an oceanic or terrestrial origin at high latitudes, mainly from the Arctic. Notably,
473 the 30% highest values explain 74% of eBC_{BB} at Birkenes for the actual period, hence LRT is decisive
474 not only for episodes of high concentrations but also largely explains the mean concentration. All eBC_{BB}
475 and eBC_{FF} observations included in the 70th percentile was made in winter despite the less pronounced
476 seasonality of eBC_{FF} compared to eBC_{BB} .

477 To generate a longer BB time series of OC_{BB} and EC_{BB} we combine the levoglucosan time series
478 (2008–2018) with levoglucosan/OC and levoglucosan/EC ratios derived from the BB factor of the PMF
479 analysis (Table 1; See Sect. S 5 for details). Depletion of levoglucosan by OH oxidation is more likely
480 in summer (Hoffmann et al., 2010; Yttri et al., 2014), still we assume that levels mostly reflect biomass
481 burning emissions in all seasons.



482 EC_{BB} levels were elevated in the heating season (Figure 9; Table S 16). A strong temperature
483 influence is illustrated by a 9°C difference in the 25th percentile of wintertime temperatures in 2015 (-
484 0.3°C) and 2010 (-9.3°C) (Figure S 1), which experienced the lowest (19 ng m⁻³) and the highest (84 ng
485 m⁻³) winter-time mean concentration of EC_{BB} , respectively. Winter 2010 was exceptionally cold due to
486 a negative North Atlantic Oscillation, and the only occasion when EC_{BB} exceeded EC_{FF} , with annual
487 mean EC_{BB} > 60% higher than the long-term mean. Pronounced interannual variability was seen for the
488 wood burning contribution in winter, from 21–60% to EC, with the lowest fractions occasionally
489 matched by those in spring and fall, typically ranging between 20–30%. EC_{BB}/EC was small in summer
490 (4–15%), considerably less than other seasons, except in 2008, where we calculate a substantial 30–40%
491 contribution. Levoglucosan cannot be used to differentiate emissions from residential wood burning,
492 wildfires and agricultural fires; exceptions are major wildfire and agricultural fire episodes identifiable
493 by unusual high concentrations and traced by source receptor models/satellite data for plumes/burnt
494 areas (Yttri et al., 2007a, Stohl et al., 2007). Influence from major wildfires in Eastern Europe caused a
495 summertime peak in fine OC and EC in 2002 at Birkenes (Yttri et al., 2007a). In June 2008, the largest
496 wildfire in Norway since the Second World War raged 25 km northeast of the Birkenes Observatory,
497 with an area of 30 km² burnt. The observatory was downwind of the fire on only one day, according to
498 FLEXPART (Figure S 2). Despite this, the levoglucosan concentration for the weekly filter sample was
499 153 ng m⁻³, by far the highest in one decade of sampling. Notably, the annual mean concentration of
500 levoglucosan for 2008 increased by nearly 35% and EC_{bb} contributed significantly to EC for summer
501 2008.

502 The seasonality of OC_{BB} (Figure 9) was like EC_{bb} . Mean wintertime OC_{BB}/OC was 39–40% and
503 >50% in 2010 and 2012, considering both PM_{10} and $PM_{2.5}$. The summertime contribution was typically
504 <5%, reflecting both low levoglucosan levels and major influences from BSOA and PBAP, which peak
505 in summer. Notably, five of the seven highest weekly OC concentrations for the PM_{10} time-series were
506 attributed to emissions from major wildfires in Eastern Europe, i.e., August 2002, and May/September
507 2006, and thus prior to the initiation of the levoglucosan time series. The local wildfire episode in
508 summer 2008 caused a substantial increase in OC_{bb}/OC (13–18%), which is within the lower range of
509 that observed for spring (12–27%) and fall (13–39%).

510

511 3.2.2 Biogenic carbonaceous aerosol sources

512 The general lack of PBAP tracers in the MIN (<1%) and SS (<2%) factors and no sea salt and Ti in the
513 PBAP factor, implies that soil and sea spray aerosol do not contribute to PBAP at Birkenes, although
514 this has been shown elsewhere (O'Dowd et al., 2004; Jia and Fraser, 2011). PBAP represented by
515 glucose, arabitol and mannitol appears to be associated with leaves rather than soil material and to be a
516 source of local origin (Samaké et al., 2019). However, even large PBAP, such as birch pollen (avg. diam.
517 22 µm), has a potential for long range atmospheric transport of 1000 km due to its low density,
518 hydrophobic nature, release during favourable dispersion conditions, and (often) emission height > 10



519 m (e.g. Sofiev et al., 2006; Skjøth et al., 2007).

520 The PBAP factor concentration was nearly one order of magnitude higher in summer and fall
521 than in winter and was the major contributor to coarse OC for all seasons except winter, particularly in
522 summer (54%) and fall (69%) (Figure 8). These are conservative estimates, as 3–9% of the PBAP tracers
523 reside in the BSOA_{SRT} factor, likely due to co-variability, as there is no scientific evidence linking
524 biologically formed sugars and sugar-alcohols to abiotic formation of BSOA. Notably, the PBAP factor
525 explained 20–26% of fine OC in summer and fall, being the major contributor in fall. Consequently,
526 PBAP was the major contributor to OC even in PM₁₀ in summer (31%) and fall (40%). The PBAP factor
527 even explained 16% of fine OC (Figure 8) annually, corresponding to 0.084 μg C m⁻³, which is
528 marginally lower than the factor's content of coarse OC (0.113 μg C m⁻³). Combined, this made PBAP
529 the most abundant contributor to OC in PM₁₀ along with the MIN factor (both 26%). Some PBAP tracers
530 partly reside in the fine mode (Carvalho et al., 2003); Yttri et al., 2007b) but the 43% OC_{PBAP} found in
531 the fine fraction in the present study is higher than what has previously been reported for the actual
532 PBAP tracers at Birkenes; i.e. 6–7% (arabitol and mannitol), 20% (trehalose), and 33% (glucose) (Yttri
533 et al., 2007b). It cannot be excluded that the PBAP factor contains some fine OC from other sources e.g.
534 due to condensation, but although there is a seasonal co-variability with the BSOA_{SRT} factor, only 2–
535 3% of the 2-methyltetrosols were explained by the PBAP factor and there was a low correlation between
536 the PBAP and the BSOA_{SRT}, which questions this hypothesis.

537 Arabitol and mannitol are well-known tracers of fungal spores (Bauer et al., 2008), one of the
538 most abundant sources of PBAP (Elbert et al., 2007). Applying an OC to mannitol ratio of 5.2–10.8 for
539 fungal spores (Bauer et al., 2008; Yttri et al., 2011a), we estimate that 11–22% of OC_{PBAP} (in PM₁₀)
540 comes from this source. Glucose is one of the primary molecular energy sources for plants and animals,
541 a building block of natural dimers and polymers (e.g. sucrose and cellulose), and thus ubiquitous in
542 nature and considered a PBAP tracer of general character, and clearly important for allocation of carbon
543 mass to PBAP. Nevertheless, a wider range of organic tracers ought to be tested in future PMF studies
544 to explore the potential of further separation of the highly heterogenic PBAP source, including cellulose,
545 but also amino acids. A greater diversity of PBAP tracers may also provide a more correct PBAP
546 estimate. The PMF approach used in the present study gives a somewhat higher, but overlapping,
547 estimate of OC_{PBAP} at Birkenes for August 2016–2018 than Latin Hypercube sampling (LHS) for August
548 2009 (Yttri et al., 2011b) (Table 3). The LHS approach was based on *a priori* emission ratios, with
549 uncertainty ranges estimated in a similar way to a Monte Carlo analysis (though less computationally
550 extensive), and considered only the sum of fungal spores and plant debris as OC_{PBAP}, based on mannitol
551 (fungal spores) and cellulose (plant debris), whereas the PMF approach may pick other contributing, i.e.
552 co-varying, sources.

553 The 3% EC in the PBAP factor is substantially less than the 16% reported by Waked et al.
554 (2014), which stated that atmospheric mixing, PMF limitations and artifacts caused by thermal-optical
555 analysis could be plausible explanations. In the present study, low levels of coarse fraction EC



556 occasionally appear in summer and fall (Table S 5), following the seasonality of PBAP. This finding
557 does not exclude any of the three possibilities proposed by Waked et al., (2014), but supports the
558 suggestion by Dusek et al. (2017) that PBAP, or at least some types of PBAP, chars and evolves as
559 modern carbon EC during thermal-optical analysis. If EC_{PBAP} indeed is an analytical artefact, then
560 constraining the PBAP factor to contain no EC, as suggested by Weber et al. (2019), should be done
561 with caution, as it will wrongfully apportion pyrolytic carbon generated from PBAP as EC to another
562 source. Thus, EC_{PBAP} should rather be interpreted as OC_{PBAP} . With no EC_{SS} , no $EC_{BSOA,SRT}$ and EC_{PBAP}
563 an assumed analytical artefact, EC can be apportioned into a fossil fuel category (EC_{FF}), consisting of
564 the MIN, IND/TRA, and NH_4NO_3 factors (explains 0.2% of levoglucosan), and a non-fossil biomass
565 burning category (EC_{BB}), the BB factor. Some EC has been reported from meat cooking (Rogge et al.,
566 1991), which is a non-fossil source, but its influence is minor at Birkenes, as it has not been observed
567 based on concurrent ACSM-measurements and is not accounted for by levoglucosan.

568 Our PMF results support the use of $OC_{PM_{10-2.5}}$ as a proxy of OC_{PBAP} , which has a pronounced
569 seasonality (Figure 4) with the highest seasonal mean concentration observed in summer for 15 of the
570 studied years and in fall for the three others (Table S 5). The seasonal mean exceeded $0.5 \mu\text{g C m}^{-3}$ on
571 two occasions only; fall 2005 and fall 2006. With a few exceptions, $OC_{PM_{10-2.5}}$ contributed more than
572 30% to $OC_{PM_{10}}$ in summer and fall. The highest relative contribution (45–50%) to $OC_{PM_{10}}$ were
573 exclusively observed in fall (2004, 2005, 2006, 2008, 2014, 2017), likely reflecting a combination of
574 high $OC_{PM_{10-2.5}}$ concentrations and fine fraction OC_{BSOA} declining at this time of the year. $OC_{PM_{10-2.5}}$
575 made a substantially lower contribution to $OC_{PM_{10}}$ in winter (mean: 13%) and in spring (mean: 19%)
576 compared to summer and fall, although contributions exceeding 25% were observed in spring for certain
577 years. Notably however, the PBAP factor explains 16% of fine OC, which would not be accounted for
578 using coarse OC as a proxy of OC_{PBAP} .

579 These numbers suggest that PBAP is a major, continuous contributor to OC in PM_{10} at Birkenes
580 for a period of nearly two decades, and that it largely explains the seasonality. Estimates of PBAP levels
581 in the continental European rural background environment are largely lacking and should be undertaken
582 to explore PBAPs potential importance. With a longer vegetative season and a different climate, the
583 PBAP flux might be larger in more southerly countries, although the relative contribution might be lower
584 due higher overall OC levels. Waked et al. (2014) found that OC_{PBAP} accounted for 17% of OC in PM_{10}
585 on an annual basis for an urban background site in Lens (Northern France), and between 5–6% in
586 winter/spring and 27–37% in summer/fall using PMF for source apportionment. These fractions are
587 comparable to those observed in the present study, albeit concentrations calculated by Waked et al.
588 (2014) were higher.

589 PBAP is a large OC source not included in many models. OC model closure, both for overall
590 levels and seasonality, would thus likely be improved in many cases by its inclusion. This appears to be
591 particularly important for regions with low anthropogenic influence. Birkenes is situated in the Boreo-
592 nemorale zone, a transition zone of the Nemorale and the Boreal zone, hence, findings made for this site



593 likely gives an indication of what can be expected for this scarcely populated, circumpolar region, which
594 by far is the largest terrestrial biome of the Northern Hemisphere. Hence, measurements in unperturbed
595 areas should include PBAP for a better understanding of background conditions. In turn, such
596 measurements may improve e.g. climate models; i.e., the aerosol climate effect under relatively clean
597 conditions.

598 Modelled estimates suggest a 10–40% contribution of BSOA to fine OC annually at Birkenes
599 (Simpson et al., 2007; Bergström et al., 2012). Hence, the 9% contribution of $OC_{BSOA,SRT}$ to fine OC,
600 and the 13% contribution to coarse OC (10% to OC in PM_{10}) found in the present study by PMF, appears
601 to be in the lower range. Further, 3–9% of the PBAP tracers reside in the $BSOA_{SRT}$ factor, hence some
602 of its OC content may rather be attributed to PBAP, further lowering the OC content of the $BSOA_{SRT}$
603 factor but strengthening coarse OC as a proxy of PBAP. $BSOA_{SRT}$ made a negligible contribution to
604 fine, coarse and PM_{10} OC in all seasons, except in summer (22–25%), apparently contradicting previous
605 studies that unambiguously points to BSOA as the major carbonaceous aerosol source at Birkenes in the
606 vegetative season (Simpson et al., 2007; Yttri et al., 2011b). Note that a prevailing BSOA source in
607 summer is considered a normal situation also for European rural background environment in general
608 (e.g. Gelencser et al., 2007), not only for Birkenes. Table 3 shows that $OC_{BSOA,SRT}$ obtained by PMF for
609 August 2016–2018 is substantially lower than that obtained by LHS for August 2009 (Yttri et al.,
610 2011b). Although not obtained for the same year, we argue that methodology rather than climatology
611 explains most of the difference. $OC_{BSOA,LHS}$ provides an upper estimate including all modern carbon,
612 local and from LRT (excluding biomass burning and PBAP fungal spores and plant debris), whereas
613 $OC_{BSOA,SRT}$ gives a lower estimate accounting for locally formed BSOA.

614 It is less likely that anthropogenic secondary organic aerosol (ASOA) resides in the $BSOA_{SRT}$ -
615 factor, as ASOA precursors result from combustion processes and evaporative losses. Further, Yttri et
616 al. (2011a) found higher ASOA concentrations in the Norwegian rural background environment in
617 winter compared to summer, which is opposite of $BSOA_{SRT}$, hence co-variation and/or apportionment
618 to the same factor do not appear likely. ASOA is less abundant than BSOA at Birkenes, as calculated
619 by Simpson et al. (2007) and Bergström et al. (2012) but the estimates vary substantially and are very
620 uncertain (Spracklen et al., 2011), particularly for ASOA (from 1% to 10–20%). It is difficult to predict
621 which PMF factor(s) accounted for ASOA, but for the sake of separating OC into a natural and an
622 anthropogenic fraction we assume that ASOA is not part of neither $BSOA_{SRT}$ nor the PBAP factor,
623 which we consider as exclusively natural factors. To provide an upper estimate of the natural sources
624 (Figure 8), we neither consider it part of the MIN factor.

625 With 90% (in PM_{10}) and 92% (in $PM_{2.5}$) of the MIN factor's OC content attributed to LRT
626 BSOA ($OC_{BSOA,LRT}$) (See Sect. 2.4.1), the combined contribution of locally formed BSOA ($OC_{BSOA,SRT}$)
627 and $OC_{BSOA,LRT}$ to OC in PM_{10} and $PM_{2.5}$ would be 34–38% on an annual basis, 37–41% in spring and
628 50–57% in summer. From this we can deduct that 1/3 of BSOA is of local origin, whereas 2/3 are long-
629 range transported. For August 2016–2018, the joint contribution of $OC_{BSOA,SRT}$ and $OC_{BSOA,LRT}$ to OC in



630 PM₁₀ is 31%, corresponding better with the LHS estimate (Table 3) but still noticeably lower. Notably,
631 OC_{BSOA,SRT}, OC_{BSOA,LRT} and OC_{PBAP} combined contributed 79% to OC in PM₁₀ in August 2016–2018,
632 which exactly matches the sum of OC_{BSOA,LHS} and OC_{PBAP,LHS} to OC in PM₁₀ in August 2009. This
633 suggests that LHS and PMF apportion an equally large amount of OC to natural sources but that the
634 split between BSOA and PBAP likely differ. It is evident that the LHS-approach provides an upper
635 estimate of BSOA (Gelenscer et al., 2007; Yttri et al. 2011a), whereas the great diversity of PBAP likely
636 is underestimated by just accounting for plant debris and fungal spores. The lower estimate of OC_{BSOA}
637 and the higher estimate of OC_{PBAP} provided by PMF in the present study is in line with this and
638 encourage further effort to apportion these major carbonaceous aerosol sources correctly. Inclusion of
639 monoterpene and sesquiterpene oxidation products (Kleindienst et al., 2007) to PMF would possibly
640 improve our understanding of the SOA apportionment, as would knowledge about their atmospheric
641 lifetime.

642

643 4. Conclusions

644 The carbonaceous aerosol time-series at the Birkenes Observatory initiated in 2001 is unique due to its
645 unprecedented length in Europe and because measurements are performed both for PM₁₀ and PM_{2.5}.
646 Such long-time series are of utmost importance, e.g. for the evaluation of projections, air-quality models,
647 and climate models. The need for concurrent and diverse off-line and on-line carbonaceous aerosol
648 speciation measurements for understanding of carbonaceous aerosol sources, seasonal, annual, and long-
649 term variability has been utterly demonstrated.

650 Statistically significant and comparably large reductions ($\sim -4\%$ yr⁻¹) were calculated for EC
651 and PM_{2.5} at the Birkenes Observatory for 2001–2018, with EC reductions largely attributed to road
652 transportation. No significant declining trend was calculated for OC, likely because prevailing natural
653 sources masked any reduction in anthropogenic sources. Further reduction of carbonaceous aerosol may
654 be hampered by poorly abated sources such as domestic heating, though more work is needed to assess
655 this. The OC fraction of PM₁₀ (+2.3% yr⁻¹) and PM_{2.5} (+3.2% yr⁻¹) increased significantly from 2001–
656 2018, whereas the EC fraction decreased ($-4.0 - -4.7\%$ yr⁻¹), causing a successive change in the aerosol
657 chemical composition and in the relative source composition.

658 Source apportionment using PMF identified seven factors, six of which were carbonaceous
659 dominated: Mineral dust dominated (MIN), traffic/industrial-like (TRA/IND), biogenic secondary
660 organic aerosol (BSOA), primary biological aerosol particles (PBAP), biomass burning (BB) and
661 ammonium nitrate dominated (NH₄NO₃). Carbonaceous material was negligible in the sea salt (SS)
662 factor. Combustion of fossil fuel (78%) was the major source of EC and TRA/IND (50%) the key factor.
663 Emissions from residential wood burning increased in the heating season but fossil fuel sources
664 dominated EC even in winter (66%). Continental Europe and western parts of Russia were the main
665 source regions of elevated levels of eBC, both for biomass burning and for combustion of fossil fuels.
666 Natural sources dominated both fine (53%) and coarse (78%) fraction OC, thus also OC in PM₁₀ (60%).



667 The natural fraction increased substantially in the vegetative season due to biogenic secondary organic
668 aerosol and primary biological aerosol particles, confined to the BSOA, PBAP and MIN factors. 77–
669 91% of OC was attributed to natural sources in summer and 22–37% in winter. The coarse fraction
670 showed the highest share of natural sources regardless of season and was dominated by PBAP, except
671 in winter. Notably, PBAP (26%) made a larger contribution to OC in PM₁₀ than BB (14%), and an
672 equally large contribution as BB (17%) in PM_{2.5}.

673

674 **Author contribution**

675 Conceptualization, Methodology and Writing – Original draft, Visualization: **Wenche Aas, Stephen M.**
676 **Platt, Xin Wan, Karl Espen Yttri**; Data Curation: **Markus Fiebig, Hans Gundersen, Anne-Gunn**
677 **Hjellbrekke, Hilde Uggerud, Marit Vadset, Karl Espen Yttri**; Formal Analysis: **Stephen M. Platt,**
678 **Sverre Solberg, Xin Wan, Karl Espen Yttri**; Funding acquisition: **Wenche Aas; Kjetil Tørseth**;
679 Resources: **Jason Surratt**; Software: **Francesco Canonaco, Sabine Eckhardt, Nikolaos Evangeliou,**
680 **Stephen M. Platt, André S. H. Prévôt**; Writing, review and editing: **Wenche Aas, Francesco**
681 **Canonaco, Sabine Eckhardt, Nikolaos Evangeliou, Markus Fiebig, Hans Gundersen, Anne-Gunn**
682 **Hjellbrekke, Cathrine Lund Myhre, Stephen M. Platt, André S. H. Prévôt, David Simpson, Sverre**
683 **Solberg, Jason Surratt, Kjetil Tørseth, Hilde Uggerud, Marit Vadset, Xin Wan, Karl Espen Yttri**

684

685 **Acknowledgements**

686 Time series used in the present study, except for the organic tracers, were obtained as part of the
687 Norwegian national monitoring program (Aas et al., 2020). The monosaccharide anhydrides, the sugar-
688 alcohols and the 2-methyltetrols (organic tracers) time series were funded by the Norwegian Research
689 Council through the Strategic Institute Projects “*Observation and Modelling Capacities for Northern*
690 *and Polar Climate and Pollution*” and the “*Studying sources, formation and transport of short-lived*
691 *climate forcers by advanced high-time resolution measurements*”. All data are reported to the EMEP
692 monitoring programme (Tørseth et al., 2012) and are available from the database infrastructure EBAS
693 (<http://ebas.nilu.no/>) hosted at NILU.

694 The research leading to these results has benefited from Aerosols, Clouds, and Trace gases
695 Research InfraStructure (ACTRIS), funding from the European Union Seventh Framework Programme
696 (FP7/2007–2013) under ACTRIS-2 and the grant agreement no. 262254, and the COST Action
697 CA16109, Chemical On-Line cOmpoSition and Source Apportionment of fine aerosol-COLOSSAL;
698 I.e., for participation in interlaboratory comparison for thermal-optical analysis and QA/QC of
699 measurements.

700 OC/EC and mass concentration were measured as part of the Norwegian national monitoring
701 programme (Aas et al., 2020), whereas monosaccharide anhydrides were analysed as part of the SACC
702 (Strategic Aerosol Observation and Modelling Capacities for Northern and Polar Climate and Pollution)
703 and SLCF (Describing sources, formation, and transport of short lived climate forcers using advanced,



704 novel measurement techniques) projects.

705

706 **References**

707 Aas, Wenche., Eckhardt, Sabine, Fiebig, Markus, Solberg, Sverre, and Yttri, Karl Espen.: Monitoring
708 of long-range transported air pollutants in Norway, annual report 2019. Kjeller, NILU (Miljødirektoratet
709 rapport, M-1710/2020) (NILU OR, 4/2020), 2020.

710

711 Aas, W., Mortier, A., Bowersox, V., Cherian, R., Faluvegi, G., Fagerli, H., Hand, J., Klimont, Z., Galy-
712 Lacaux, C., Lehmann, C. M. B., Myhre, C. L., Myhre, G., Olivie, D., Sato, K., Quaas, J., Rao, P. S. P.,
713 Schulz, M., Shindell, D., Skeie, R. B., Stein, A., Takemura, T., Tsyro, S., Vet, R., and Xu, X.: Global
714 and regional trends of atmospheric sulfur, *Sci Rep* 9, 953 (2019), <https://doi.org/10.1038>.

715

716 Alastuey, A., Querol, X., Aas, W., Lucarelli, F., Pérez, P., Moreno, T., Cavalli, F., Areskoug, H., Balan,
717 V., Catrambone, M., Ceburnis, D., Cerro, J. C., Conil, S., Gevorgyan, L., Hueglin, C., Imre, K., Jaffrezo,
718 J.-L., Leeson, S. R., Mihalopoulos, N., Mitisinkova, M., O'Dowd, C. D., Pey, J., Putaud, J.-P., Riffault,
719 V., Ripoll, A., Sciare, J., Sellegri, K., Spindler, G., and Yttri, K. E.: Geochemistry of PM₁₀ over Europe
720 during the EMEP intensive measurement periods in summer 2012 and winter 2013, *Atmos. Chem.*
721 *Phys.*, 16, 6107–6129, 2016, doi:10.5194/acp-16-6107-2016.

722

723 Bauer, H., Kasper-Giebl, A., Lound, M., Giebl, H., Hitzemberger, R., Zibuschka, F., and Puxbaum, H.:
724 The contribution of bacteria and fungal spores to the organic carbon content of cloud water, precipitation
725 and aerosols, *Atmos. Res.*, 64, 109-119, 2002.

726

727 Bauer, H., Claeys, M., Vermeylen, R., Schueller, E., Weinke, G., Berger, A., and Puxbaum, H.: Arabitol
728 and mannitol as tracers for the quantification of airborne fungal spores, *Atmos. Environ.*, 42, 3, January
729 2008, Pages 588-593.

730

731 Bergström, R., Denier van der Gon, H. A. C., Prévôt, A. S. H., Yttri, K. E., and Simpson, D.: Modelling
732 of organic aerosols over Europe (2002–2007) using a volatility basis set (VBS) framework: application
733 of different assumptions regarding the formation of secondary organic aerosol, *Atmos. Chem. Phys.*, 12,
734 8499–8527, 2012.

735

736 Birch, M. E. and Cary, R. A.: Elemental Carbon-Based Method for Monitoring Occupational Exposures
737 to Particulate Diesel Exhaust, *Aerosol Sci. Technol.*, 25, 221-241, 1996.

738

739 Bond, T. C., Doherty, S. J., Fahey, D. W., Forster, P. M., Berntsen, T., DeAngelo, B. J., Flanner, M. G.,
740 Ghan, S., Kärcher, B., Koch, D., Kinne, S., Kondo, Y., Quinn, P. K., Sarofim, M. C., Schultz, M. G.,



- 741 Schulz, M., Venkataraman, C., Zhang, H., Zhang, S., Bellouin, N., Guttikunda, S. K., Hopke, P. K.,
742 Jacobson, M. Z., Kaiser, J. W., Klimont, Z., Lohmann, U., Schwarz, J. P., Shindell, D., Storelvmo, T.,
743 Warren, S. G., Zender, C. S.: Bounding the role of black carbon in the climate system: a scientific
744 assessment, *J. Geophys. Res. Atmos.* 118, 5380–5552, <https://doi.org/10.1002/jgrd.50171>, 2013.
- 745
- 746 Boucher, O., Randall, D., Artaxo, P., Bretherton, C., Feingold, G., Forster, P., Kerminen, V.-M., Kondo,
747 Y., Liao, H., Lohmann, U., Rasch, P., Satheesh, S. K., Sherwood, S., Stevens, B., and Zhang, X.Y.:
748 Clouds and Aerosols. In: *Climate Change 2013: The Physical Science Basis. Contribution of Working*
749 *Group I to the Fifth Assessment Report of the Intergovernmental Panel on Climate Change* [Stocker,
750 T.F., Qin, D., Plattner, G. K., Tignor, M., Allen, S. K., Boschung, J., Nauels, A., Xia, Y., Bex, V., and
751 Midgley, P. M. (eds.)]: Cambridge University Press, Cambridge, United Kingdom and New York, NY,
752 USA, 2013.
- 753
- 754 A. Bougiatioti, Stavroulas, I., Kostenidou, E., Zarpas, P., Theodosi, C., Kouvarakis, G., Canonaco,
755 F., Prévôt, A. S. H., Nenes, A., Pandis, S. N., and Mihalopoulos, N.: Processing of biomass-burning
756 aerosol in the eastern Mediterranean during summertime. *Atmos. Chem. Phys.*, 14, 4793–4807, 2014.
- 757
- 758 Canonaco, F., M. Crippa, J. G. Slowik, U. Baltensperger, and A. S. H. Prevot. SoFi, an IGOR-based
759 interface for the efficient use of the generalized multilinear engine (ME-2) for the source apportionment:
760 ME-2 application to aerosol mass spectrometer data, *Atmospheric Measurement Techniques*, 6(12),
761 3649-3661, 2013.
- 762
- 763 Carvalho, A., Pio, C., and Santos, C.: Water-soluble hydroxylated organic compounds in German and
764 Finnish aerosols, *Atmos. Environ.*, 37, 1775–1783, 2003.
- 765
- 766 Cassiani, M., Stohl, A., and Brioude, J.: Lagrangian Stochastic Modelling of Dispersion in the
767 Convective Boundary Layer with Skewed Turbulence Conditions and a Vertical Density Gradient:
768 Formulation and Implementation in the FLEXPART Model, *Boundary-Layer Meteorol.*, 154(3), 367–
769 390, doi:10.1007/s10546-014-9976-5, 2014.
- 770
- 771 Cattiaux, J., Vautard, R., Cassou, C., Yiou, P., Masson-Delmotte, V., and Codron, F.: Winter 2010 in
772 Europe: A cold extreme in a warming climate. *Geophysical Research Letters*, 37, L20704.
773 <https://doi.org/10.1029/2010GL044613>, 2010.
- 774
- 775 Cavalli, F., Viana, M., Yttri, K. E., Genberg, J., and Putaud, J.-P.: Toward a standardized thermal-optical
776 protocol for measuring atmospheric organic and elemental carbon: the EUSAAR protocol, *Atmos.*
777 *Meas. Tech.*, 3, 79–89, doi:10.5194/amt-3-79-2010, 2010.



778
779 Cavalli, F., Putaud, J.-P., and Yttri, K. E.: Availability and quality of the EC and OC measurements
780 within EMEP, including results of the fourth interlaboratory comparison of analytical methods for
781 carbonaceous particulate matter within EMEP (2011), NILU, Kjeller, EMEP/CCC-report 1/2013, 2013.
782
783 <https://www.ceip.at>
784
785 Claeys, M., Graham, B., Vas, G., Wang, W., Vermeylen, R., Pashynska, V., Cafmeyer, J., Guyon, P.,
786 Andreae, M. O., Artaxo, P., and Maenhaut, W.: Formation of secondary organicaerosols through
787 photooxidation of isoprene, *Science*, 303, 1173–1176, 2004.
788
789 Crippa, M., Canonaco, F., Lanz, V. A., Äijälä, M., Allan, J. D., Carbone, S., Capes, G., Ceburnis, D.,
790 Dall'Osto, M., Day, D. A., DeCarlo, P. F., Ehn, M., Eriksson, A., Freney, E., Hildebrandt Ruiz, L.,
791 Hillamo, R., Jimenez, J. L., Junninen, H., Kiendler-Scharr, A., Kortelainen, A.-M., Kulmala, M.,
792 Laaksonen, A., Mensah, A. A., Mohr, C., Nemitz, E., O'Dowd, C., Ovadnevaite, J., Pandis, S. N., Petäjä,
793 T., Poulain, L., Saarikoski, S., Sellegri, K., Swietlicki, E., Tiitta, P., Worsnop, D. R., Baltensperger, U.,
794 and Prévôt, A. S. H.: Organic aerosol components derived from 25 AMS data sets across Europe using
795 a consistent ME-2 based source apportionment approach, *Atmos. Chem. Phys.*, 14, 6159–6176,
796 <https://doi.org/10.5194/acp-14-6159-2014>, 2014.
797
798 Denier van der Gon, H. A. C., Bergström, R., Fountoukis, C., Johansson, C., Pandis, S. N., Simpson,
799 D., and Visschedijk, A. J. H.: Particulate emissions from residential wood combustion in Europe –
800 revised estimates and an evaluation, *Atmos. Chem. Phys.*, 15, 6503–6519, [https://doi.org/10.5194/acp-](https://doi.org/10.5194/acp-15-6503-2015)
801 [15-6503-2015](https://doi.org/10.5194/acp-15-6503-2015), 2015.
802
803 Donahue, N. M., Robinson, A. L., and Pandis, S. N.: Atmospheric organic particulate matter: From
804 smoke to secondary organic aerosol, *Atmospheric Environment – Fifty Years of Endeavour*, *Atmos.*
805 *Environ.*, 43, 94–106, doi:10.1016/j.atmosenv.2008.09.055, 2009.
806
807 Dusek, U., Hitenberger, R., Kasper-Giebl, A., Kistler, M., Meijer, H. A. J., Szidat, S., Wacker, L.,
808 Holzinger, R., and Röckmann, T.: Sources and formation mechanisms of carbonaceous aerosol at a
809 regional background site in the Netherlands: insights from a year-long radiocarbon study, *Atmos. Chem.*
810 *Phys.*, 17, 3233–3251, <https://doi.org/10.5194/acp-17-3233-2017>, 2017.
811
812 Dye, C. and Yttri, K. E.: Determination of monosaccharide anhydrides in atmospheric aerosols by use
813 of high-resolution mass spectrometry combined with high performance liquid chromatography, *Anal.*
814 *Chem.*, 77, 1853–1858, 2005.



815
816 EEA, 2020: Long term air quality measurements trends in Europe. In prep.
817
818 Elbert, W., Taylor, P. E., Andreae, M. O., and Pöschl, U.: Contribution of fungi to primary biogenic
819 aerosols in the atmosphere: wet and dry discharged spores, carbohydrates, and inorganic ions. *Atmos.*
820 *Chem. Phys.*, 7, 4569–4588, 2007.
821
822 Fine, P. M., Cass, G. R., and Simoneit, B. R. T.: Chemical characterization of fine particle emissions
823 from the fireplace combustion of woods grown in the Northeastern United States, *Environ. Sci.*
824 *Technol.*, 35, 2665–2675, 2001.
825
826 Fine, P. M., Cass, G. R., and Simoneit, B. R. T.: Chemical characterization of fine particle emissions
827 from the fireplace combustion of woods grown in the Southern United States, *Environ. Sci. Technol.*,
828 36, 1442–1451, 2002a.
829
830 Fine, P. M., Cass, G. R., and Simoneit, B. R. T.: Organic compounds in biomass smoke from residential
831 wood combustion: Emissions characterization at a continental scale, *J. Geophys. Res.*, 107, D8349,
832 doi:10.1029/2001JD000661, 2002b.
833
834 Fine, P. M., Cass, G. R., and Simoneit, B. R. T.: Chemical characterization of fine particle emissions
835 from the fireplace combustion of wood types grown in the Midwestern and Western United States,
836 *Environ. Eng. Sci.*, 21, 387–409, 2004.
837
838 Fomba, K. W., Pinxteren, D. van, Müller, K., Spindler, G., and Herrmann, H.: Assessment of trace metal
839 levels in size-resolved particulate matter in the area of Leipzig, *Atmos Environ.*, 176, 60 – 70,
840 <https://doi.org/10.1016/j.atmosenv.2017.12.024>, 2018.
841
842 Forster, C., Stohl, A., and Seibert, P.: Parameterization of convective transport in a Lagrangian particle
843 dispersion model and its evaluation, *J. Appl. Meteorol. Climatol.*, 46(4), 403–422,
844 doi:10.1175/JAM2470.1, 2007.
845
846 Fröhlich-Nowoisky, J., Kampf, C. J., Weber, B., Huffman, J. A., Pöhlker, C., Andreae, M. O., Lang-
847 Yona, N., Burrows, S. M., Gunthe, S. S., Elbert, W., Su, H., Hoor, P., Thines, E., Hoffmann, T., Després,
848 V. R., and Pöschl, U.: Bioaerosols in the Earth system: Climate, health, and ecosystem interactions,
849 *Atmospheric Research* 182, 346 – 376, 2016.
850



- 851 Fuller, G. W., Tremper, A. H., Baker, T. D., Yttri, K. E., and Butterfield, D.: Contribution of wood
852 burning to PM₁₀ in London, *Atmos. Environ.*, 87, 87–94,
853 <https://doi.org/10.1016/j.atmosenv.2013.12.037>, 2014.
854
- 855 Gelencsér, A., May, B., Simpson, D., Sánchez-Ochoa, A., Kasper-Giebl, A., Puxbaum, H., Caseiro, A.,
856 Pio, C., and Legrand, M.: Source apportionment of PM_{2.5} organic aerosol over Europe:
857 primary/secondary, natural/anthropogenic, fossil/biogenic origin, *J. Geophys. Res.*, 112, D23S04,
858 <https://doi.org/10.1029/2006JD008094>, 2007.
859
- 860 Genberg, J., Hyder, M., Stenström, K., Bergström, R., Simpson, D., Fors, E. O., Jönsson, J. Å., and
861 Swietlicki, E.: Source apportionment of carbonaceous aerosol in southern Sweden, *Atmos. Chem. Phys.*,
862 11, 11387–11400, <https://doi.org/10.5194/acp-11-11387-2011>, 2011.
863
- 864 Gilardoni, S., Vignati, E., Cavalli, F., Putaud, J. P., Larsen, B. R., Karl, M., Stenström, K., Genberg, J.,
865 Henne, S., and Dentener, F.: Better constraints on sources of carbonaceous aerosols using a combined
866 ¹⁴C – macro tracer analysis in a European rural background site, *Atmos. Chem. Phys.*, 11, 5685–5700,
867 <https://doi.org/10.5194/acp-11-5685-2011>, 2011.
868
- 869 Glasius, M., Hansen, A. M. K., Claeys, M., Henzing, J. S., Jedynska, A. D., Kasper-Giebl, A., Kistler,
870 M., Kristensen, K., Martinsson, J., Maenhaut, W., Nøjgaard, J., Spindler, G., Stenström, K. E.,
871 Swietlicki, E., Szidat, S., Simpson, D., and Yttri, K. E.: Composition and sources of carbonaceous
872 aerosols in Northern Europe during winter, *Atmos. Environ.*, 173, 127–141,
873 <https://doi.org/10.1016/j.atmosenv.2017.11.005>, 2018.
874
- 875 Grythe, H., Kristiansen, N. I., Groot Zwaafink, C. D., Eckhardt, S., Ström, J., Tunved, P., Krejci, R.
876 and Stohl, A.: A new aerosol wet removal scheme for the Lagrangian particle model FLEXPARTv10,
877 *Geosci. Model Dev.*, 10, 1447–1466, doi:10.5194/gmd-10-1447-2017, 2017.
878
- 879 Grythe, H., Lopez-Aparicio, S., Vogt, M., Vo Thanh, D., Hak, C., Halse, A. K., Hamer, P., and Sousa
880 Santos, G.: The MetVed model: development and evaluation of emissions from residential wood
881 combustion at high spatio-temporal resolution in Norway, *Atmos. Chem. Phys.*, 19, 10217–10237,
882 <https://doi.org/10.5194/acp-19-10217-2019>, 2019.
883
- 884 Hallquist, M., Wenger, J. C., Baltensperger, U., Rudich, Y., Simpson, D., Claeys, M., Dommen, J.,
885 Donahue, N. M., George, C., Goldstein, A. H., Hamilton, J. F., Herrmann, H., Hoffmann, T., Iinuma,
886 Y., Jang, M., Jenkin, M. E., Jimenez, J. L., Kiendler-Scharr, A., Maenhaut, W., McFiggans, G.,
887 Mentel, Th. F., Monod, A., Prevot, A. S. H., Seinfeld, J. H., Surratt, J. D., Szmigielski, R., and Wildt,



- 888 J.: The formation, and impact of secondary organic aerosol: current and emerging issues, *Atmos.*
889 *Chem. Phys.*, 9, 5155–5236, doi:10.5194/acp-9-5155-2009, 2009.
- 890
- 891 Herich, H., M. F. D. Gianini, C. Piot, G. Mocnik, J. L. Jaffrezo, J. L. Besombes, A. S. H. Prevot, and C.
892 Hueglin. Overview of the impact of wood burning emissions on carbonaceous aerosols and PM in large
893 parts of the Alpine region, *Atmospheric Environment*, 89, 64-75, 2014.
- 894
- 895 Hirdman, D., Sodemann, H., Eckhardt, S., Burkhardt, J. F., Jefferson, A., Mefford, T., Quinn, P. K.,
896 Sharma, S., Ström, J., and Stohl, A.: Source identification of short-lived air pollutants in the Arctic using
897 statistical analysis of measurement data and particle dispersion model output, *Atmos. Chem. Phys.*, 10,
898 669–693, 2010.
- 899
- 900 Hjellbrekke, A-G.: Data Report 2018. Particulate matter, carbonaceous and inorganic compounds,
901 NILU, Kjeller, EMEP/CCC-Report 1/2020, 2020
- 902
- 903 Hodnebrog, Ø., Myhre, G., and Samset, B.: How shorter black carbon lifetime alters its climate effect
904 *Nature Communications* 5, <https://doi.org/10.1038/ncomms6065>, 2014.
- 905
- 906 Hoffmann, D., Tilgner, A., Iinuma, Y., and Herrmann, H.: Atmospheric stability of levoglucosan: a
907 detailed laboratory and modeling study, *Environ. Sci. Technol.*, 44, 694–699, doi:10.1021/es902476f,
908 2010.
- 909
- 910 Hu, Y., Fernandez-Anez, N., Smith, T. E. L. and Rein, G.: Review of emissions from smouldering
911 peat fires and their contribution to regional haze episodes, *Int. J. Wildl. Fire*, 27(5), 293–312,
912 doi:10.1071/WF17084, 2018.
- 913
- 914 Janssen, N. A. H., Gerlofs-Nijland, M. E., Lanki, T., Salonen, R. O., Cassee, F., Hoek, G., Fischer, P.,
915 Brunekreef, B., and Krzyzanowski, M.: Health effects of black carbon. Copenhagen: WHO Regional
916 Office for Europe, 2012.
- 917
- 918 Jia, Y. and Fraser, M.: Characterization of Saccharides in Size-fractionated Ambient Particulate Matter
919 and Aerosol Sources: The Contribution of Primary Biological Aerosol Particles (PBAPs) and Soil to
920 Ambient Particulate Matter, *Environ. Sci. Technol.*, 45,3, 930 – 936, 2011.
- 921
- 922 Jordan, T. B. and Seen, A.J.: Effect of airflow setting on the organic composition of woodheater
923 emissions, *Environmental Science and Technology*, 39 (10), pp. 3601-361, 2005.
- 924



- 925 Kahnert, M., Lazaridis, M., Tsyro, S., and Tørseth, K.: Requirements for developing a regional
926 monitoring capacity for aerosols in Europe within EMEP, *J. Environ. Monitor.*, 6, 646–655, 2004.
927
- 928 Kleindienst, T. E., Jaoui, M., Lewandowski, M., O_{en}berg, J. H., Lewis, C. W., Bhave, P. V., and Edney,
929 E. O.: Estimates of the contributions of biogenic and anthropogenic hydrocarbons to secondary organic
930 aerosol at a southeastern US location, *Atmos. Environ.*, 41, 8288–8300, 2007.
931
- 932 Kyllönen, K., Vestenius, M., Anttila, P., Makkonen, U., Aurela, M., Wängberg, I., Nerentorp
933 Mastromonaco, M., and Hakola, H.: Trends and source apportionment of atmospheric heavy metals at
934 a subarctic site during 1996–2018, *Atmos. Environ.* 236, 117644.
935 <https://doi.org/10.1016/j.atmosenv.2020.117644>, 2020.
936
- 937 Lanz, V. A., Prévôt, A. S. H., Alfarra, M. R., Weimer, S., Mohr, C., DeCarlo, P. F., Gianini, M. F. D.,
938 Hueglin, C., Schneider, J., Favez, O., D’Anna, B., George, C., and Baltensperger, U.: Characterization
939 of aerosol chemical composition with aerosol mass spectrometry in Central Europe: an overview,
940 *Atmos. Chem. Phys.*, 10, 10453–10471, doi:10.5194/acp-10-10453-2010, 2010.
941
- 942 Long, C. M., Nascarella, M. A. and Valberg, P. A.: Carbon black vs. black carbon and other airborne
943 materials containing elemental carbon: Physical and chemical distinctions, *Environ. Pollut.*, 181, 271–
944 286, doi:10.1016/j.envpol.2013.06.009, 2013.
945
- 946 Lund, M. T., Myhre, G., Haslerud, A. S., Skeie, R. B., Griesfeller, J., Platt, S. M., Kumar, R., Myhre,
947 C. L., and Schulz, M.: Concentrations and radiative forcing of anthropogenic aerosols from 1750 to
948 2014 simulated with the Oslo CTM3 and CEDS emission inventory, *Geosci. Model Dev.*, 11, 4909–
949 4931, <https://doi.org/10.5194/gmd-11-4909-2018>, 2018.
950
- 951 Maenhaut, W., Vermeylen, R., Claeys, M., Vercauteren, J., Matheussen, C., and Roekens, E.
952 Assessment of the contribution from wood burning to the PM₁₀ aerosol in Flanders, Belgium, *Science
953 of the Total Environment*, 437, 226–236, 2012.
954
- 955 Matthews, B., Mareckova, K., Schindlbacher, S., Ullrich, B., and Wankmüller, R.: Emissions for 2018,
956 in: *Transboundary particulate matter, photo-oxidants, acidifying and eutrophying components. EMEP
957 Status Report 1/2020*, pp. 37–57, The Norwegian Meteorological Institute, Oslo, Norway, 2020.
958
- 959 Myhre, G., Shindell, D., Bréon, F.-M., Collins, W., Fuglestedt, J., Huang, J., Koch, D., Lamarque, J.-
960 F., Lee, D., Mendoza, B., Nakajima, T., Robock, A., Stephens, G., Takemura, T., and Zhang, H.:
961 Anthropogenic and Natural Radiative Forcing. In: *Climate Change 2013: The Physical Science Basis.*



- 962 Contribution of Working Group I to the Fifth Assessment Report of the Intergovernmental Panel on
963 Climate Change [Stocker, T.F., Qin, D., Plattner, G.-K., Tignor, M., Allen, S.K., Boschung, J., Nauels,
964 A., Xia, Y., Bex, V., and Midgley, P.M. (eds.)], Cambridge University Press, Cambridge, United
965 Kingdom and New York, NY, USA, 2013.
- 966
- 967 Myhre, G. and Samset, B. H.: Standard climate models radiation codes underestimate black carbon
968 radiative forcing, *Atmos. Chem. Phys.*, 15, 2883-2888, doi:10.5194/acp-15-2883-2015, 2015.
- 969
- 970 O’ Dowd, C. D., Facchini, M. C., Cavalli, F., Ceburnis, D., Mircea, M., Decesari, S., Fuzzi, S., Yoon, Y.
971 J., and Putaud, J. P.: Biogenically driven organic contribution to marine aerosol, *Nature*, 431, 676–680,
972 <https://doi.org/10.1038/nature02959>, 2004.
- 973
- 974 Pacyna, J. M., Nriagu, J. O., Davidson, C. I. (Eds.): *Toxic Metals in the Atmosphere*, Wiley, New
975 York, USA, (1986).
- 976
- 977 Pisso, I., Sollum, E., Grythe, H., Kristiansen, N., Cassiani, M., Eckhardt, S., Arnold, D., Morton, D.,
978 Thompson, R. L., Groot Zwaaftink, C. D., Evangelou, N., Sodemann, H., Haimberger, L., Henne, S.,
979 Brunner, D., Burkhardt, J. F., Fouilloux, A., Brioude, J., Philipp, A., Seibert, P., and Stohl, A.: The
980 Lagrangian particle dispersion model FLEXPART version 10.4, *Geosci. Model Dev.*, 12, 4955–4997,
981 doi:10.5194/gmd-12-4955-2019, 2019.
- 982
- 983 Platt et al., (in prep.). Source apportionment of equivalent black carbon from the winter 2017–2018
984 EMEP intensive measurement campaign using PMF.
- 985 Putaud, J. P., Van Dingenen, R., Alastuey, A., Bauer, H., Birmili, W., Cyrys, J., Flentje, H., Fuzzi, S.,
986 Gehrig, R., Hansson, H. C., Harrison, R., Herrmann, H., Hittenberger, R., Hüglin, C., Jones, A., Kasper-
987 Giebl, A., Kiss, G., Kousa, A., Kuhlbusch, T., Löschau, G., Maenhaut, W., Molnar, A., Moreno, T.,
988 Pekkanen, J., Perrino, C., Pitz, M., Puxbaum, H., Querol, X., Rodriguez, S., Salma, I., Schwarz, J.,
989 Smolik, J., Schneider, J., Spindler, G., ten Brink, H., Tursic, J., Viana, M., Wiedensohler, A., Raes, F.:
990 A European aerosol phenomenology - 3: Physical and chemical characteristics of particulate matter from
991 60 rural, urban, and kerbside sites across Europe, *Atmospheric Environment* 44, 1308–132, 2010.
- 992 Puxbaum, H., Caseiro, A., Sánchez-Ochoa, A., Kasper-Giebl, A., Claeys, M., Gelencsér, A., Legrand,
993 M., Preunkert, S., and Pio, C. A.: Levoglucosan levels at background sites in Europe for assessing the
994 impact of biomass combustion on the European, aerosol background, *J. Geophys. Res.*, 112, D23S05,
995 doi:10.1029/2006JD008114, 2007.
- 996



- 997 Reis, S., Grennfelt, P., Klimont, Z., Amann, M., ApSimon, H., Hettelingh, J.-P., Holland, M., LeGall,
998 A.-C., Maas, R., Posch, M., Spranger, T., Sutton, M. A., and Williams, M.: From Acid Rain to Climate
999 Change, *Science*, 338, 1153–1154, <https://doi.org/10.1126/science.1226514>, URL
1000 <http://www.sciencemag.org/content/338/6111/1153.short>, 2012.
- 1001
- 1002 A. Ripoll, Minguillón, M. C., Pey, J., Pérez, N., Querol, X., and Alastuey, A.: Joint analysis of
1003 continental and regional background environments in the western Mediterranean: PM₁ and PM₁₀
1004 concentrations and composition, *Atmos. Chem. Phys.*, 15, 1129–1145, [www.atmos-chem-](http://www.atmos-chem-phys.net/15/1129/2015/doi:10.5194/acp-15-1129-2015)
1005 [phys.net/15/1129/2015/doi:10.5194/acp-15-1129-2015](http://www.atmos-chem-phys.net/15/1129/2015/doi:10.5194/acp-15-1129-2015), 2015.
- 1006
- 1007 Rogge, W. F., Hildemann, L. M., Mazurek, M. A., Cass, G. R., and Simonelt, B. R. T.: Sources of fine
1008 organic aerosol I, Charbroilers and meat cooking operations, *Environ. Sci. Technol.* 25, 1112–1125,
1009 1991.
- 1010
- 1011 Rötzer, T. and Chmielewski, F.-M.: Phenological maps of Europe, *Climate Research*, Vol. 18: 249–257,
1012 DOI: 10.3354/cr018249, 2001.
- 1013
- 1014 Saarikoski, S., Timonen, H., Saarnio, K., Aurela, M., Järvi, L., Keronen, P., Kerminen, V.-M., and
1015 Hillamo, R.: Sources of organic carbon in fine particulate matter in northern European urban air, *Atmos.*
1016 *Chem. Phys.*, 8, 6281–6295, <https://doi.org/10.5194/acp-8-6281-2008>, 2008.
- 1017
- 1018 Saffari, A., Daher, N., Samara, C., Voutsas, D., Kouras, A., Manoli, E., Karagkiozidou, O., Vlachokostas,
1019 C., Moussiopoulos, N., Shafer, M. M., Schauer, J. J., Sioutas, C.: Increased Biomass Burning Due to the
1020 Economic Crisis in Greece and Its Adverse Impact on Wintertime Air Quality in Thessaloniki, *Environ.*
1021 *Sci. Technol.* 47, 13313–13320, doi: 10.1021/es403847h, 2013.
- 1022
- 1023 Samaké, A., Jaffrezo, J.-L., Favez, O., Weber, S., Jacob, V., Canete, T., Albinet, A., Charron, A.,
1024 Riffault, V., Perdrix, E., Waked, A., Golly, B., Salameh, D., Chevrier, F., Oliveira, D. M., Besombes,
1025 J.-L., Martins, J. M. F., Bonnaire, N., Conil, S., Guillaud, G., Mesbah, B., Rocq, B., Robic, P.-Y., Hulin,
1026 A., Le Meur, S., Descheemaeker, M., Chretien, E., Marchand, N., and Uzu, G.: Arabitol, mannitol, and
1027 glucose as tracers of primary biogenic organic aerosol: the influence of environmental factors on
1028 ambient air concentrations and spatial distribution over France, *Atmos. Chem. Phys.*, 19, 11013–11030,
1029 <https://doi.org/10.5194/acp-19-11013-2019>, 2019.
- 1030
- 1031 Sandradewi, J., Prévôt, A. S. H., Szidat, S., Perron, N., Alfarra, M. R., Lanz, V. A., Weingartner, E.,
1032 and Baltensperger, U.: Using aerosol light absorption measurements for the quantitative determination
1033 of wood burning and traffic emission contributions to particulate matter, *Environ. Sci. Technol.* 42,



- 1034 3316-3323, <https://doi.org/10.1021/es702253m>, 2008.
- 1035
- 1036 Schmidl, C., Marr, I. L., Caseiro, A., Kotianova, P., Berner, A., Bauer, H., Kasper-Giebl, A. and
1037 Puxbaum, H.: Chemical characterisation of fine particle emissions from wood stove combustion of
1038 common woods growing in mid-European Alpine regions, *Atmos. Environ.*, 42, 126–141, 2008.
- 1039
- 1040 Sciare, J., Oikonomou, K., Favez, O., Liakakou, E., Markaki, Z., Cachier, H., and Mihalopoulos, N.:
1041 Long-term measurements of carbonaceous aerosols in the Eastern Mediterranean: evidence of long-
1042 range transport of biomass burning, *Atmos. Chem. Phys.*, 8, 5551–5563, <https://doi.org/10.5194/acp-8-5551-2008>, 2008.
- 1043
- 1044
- 1045 Sillanpää M., Frey, A., Hillamo, R., Pennanen, A. S., and Salonen, R. O: Organic, elemental and
1046 inorganic carbon in particulate matter of six urban environments in Europe, *Atmos. Chem. Phys.*,
1047 2869–2879, 2005.
- 1048
- 1049 Simpson, D., Yttri, K. E., Klimont, Z., Kupiainen, K., Caseiro, A., Gelencsér, A., Pio, C., and Legrand,
1050 M.: Modeling carbonaceous aerosol over Europe, Analysis of the CARBOSOL and EMEP EC/OC
1051 campaigns, *J. Geophys. Res.*, 112, D23S14, <https://doi.org/10.1029/2006JD008114>, 2007.
- 1052
- 1053 Simpson, D., Bergström, R., Denier van der Gon, H., Kuenen, J., Schindlbacher, S., and
1054 Visschedijk, A.: Condensable organics; issues and implications for EMEP calculations and
1055 source-receptor matrices, in: Transboundary particulate matter, photo-oxidants, acidifying
1056 and eutrophying components. EMEP Status Report 1/2019, pp. 71-88, The Norwegian
1057 Meteorological Institute, Oslo, Norway, 2019.
- 1058
- 1059 Skjøth, C. A., Sommer, J., Stach, A., Smith, M., and Brandt, J.: The long-range transport of birch
1060 (*Betula*) pollen from Poland and Germany causes significant pre-season concentrations in Denmark,
1061 *Clinical and Experimental Allergy*, 37, 1204–1212, doi.org/10.1111/j.1365-2222.2007.02771.x, 2007.
- 1062
- 1063 Sofiev, M., Siljamo, P., Ranta, H., and Rantio-Lehtimäki, A.: Towards numerical forecasting of long-
1064 range air transport of birch pollen: theoretical considerations and a feasibility study, *Int J Biometeorol*
1065 50, 392, <https://doi.org/10.1007/s00484-006-0027-x>, 2006.
- 1066
- 1067 Gelencsér, A., May, B., Simpson, D., Sanchez-Ochoa, A., Kasper-Giebl, A., Puxbaum, H., Caseiro, A.,
1068 Pio, C., and Legrand, M.: Source apportionment of PM_{2.5} organic aerosol over Europe:
1069 primary/secondary, natural/anthropogenic, fossil/biogenic origin, *J. Geophys. Res.*, 112, D23S04,
1070 <https://doi.org/10.1029/2006JD008094>, 2007.



- 1071
- 1072 Stohl, A., Andrews, E., Burkhardt, J. F., Forster, C., Herber, A., Hoch, S. W., Kowal, D., Lunder, C.,
1073 Mefford, T., Ogren, J. A., Sharma, S., Spichtinger, N., Stebel, K., Stone, R., Ström, J., Tørseth, K.,
1074 Wehrli, C., and Yttri, K. E.: Pan-Arctic enhancements of light absorbing aerosol concentrations due to
1075 North American boreal forest fires during summer 2004, *J. Geophys. Res.*, 111, D22214,
1076 doi:10.1029/2006JD007216, 2006.
- 1077
- 1078 Stohl, A., Berg, T., Burkhardt, J. F., Fjæraa, A. M., Forster, C., Herber, A., Hov, Ø., Lunder, C.,
1079 McMillan, W. W., Oltmans, S., Shiobara, M., Simpson, D., Solberg, S., Stebel, K., Ström, J., Tørseth,
1080 K., Treffeisen, R., Virkkunen, K., and Yttri, K. E.: Arctic smoke – record high air pollution levels in the
1081 European Arctic due to agricultural fires in Eastern Europe in spring 2006, *Atmos. Chem. Phys.*, 7, 511–
1082 534, <https://doi.org/10.5194/acp-7-511-2007>, 2007.
- 1083
- 1084 Stohl, A., C. Forster, A. Frank, P. Seibert, and G. Wotawa : Technical Note: The Lagrangian particle
1085 dispersion model FLEXPART version 6.2, *Atmos. Chem. Phys.* 5, 2461-2474, 2005.
- 1086
- 1087 Stumm, W. and Morgan, J. J. (eds.): *Aquatic Chemistry: Chemical Equilibria and Rates in Natural*
1088 *Waters*, 3rd Edition, Wiley-Interscience Series of Texts and Monographs, Wiley, New York, 1996.
- 1089
- 1090 Szidat, S., Prévot, A. S. H., Sandradewi, J., Alfarra, M. R., Synal, H. A., Wacker, L., and Baltensperger,
1091 U.: Dominant impact of residential wood burning on particulate matter in Alpine valleys during winter.
1092 *Geophys. Res. Lett.* 34, L05820, 2007.
- 1093
- 1094 Szidat, S., Ruff, M., Perron, N., Wacker, L., Synal, H.-A., Hallquist, M., Shannigrahi, A. S., Yttri, K.
1095 E., Dye, C., and Simpson, D.: Fossil and non-fossil sources of organic carbon (OC) and elemental
1096 carbon (EC) in Göteborg, Sweden, *Atmos. Chem. Phys.*, 9, 1521–1535, doi:10.5194/acp-9-1521-2009,
1097 2009.
- 1098
- 1099 Theobald, M. R., Vivanco, M. G., Aas, W., Andersson, C., Ciarelli, G., Couvidat, F., Cuvelier, K.,
1100 Manders, A., Mircea, M., Pay, M.-T., Tsyro, S., Adani, M., Bergström, R., Bessagnet, B., Briganti, G.,
1101 Cappelletti, A., D'Isidoro, M., Fagerli, H., Mar, K., Otero, N., Raffort, V., Roustan, Y., Schaap, M.,
1102 Wind, P., and Colette, A.: An evaluation of European nitrogen and sulfur wet deposition and their trends
1103 estimated by six chemistry transport models for the period 1990–2010, *Atmos. Chem. Phys.*, 19, 379–
1104 405, <https://doi.org/10.5194/acp-19-379-2019>, 2019.
- 1105
- 1106 Turpin, B.J., Lim, H.-J.: Species contributions to PM_{2.5} mass concentrations: Revisiting common
1107 assumptions for estimating organic mass. *Aerosol Science and Technology* 35, 602-610, 2001.



- 1108
- 1109 Tørseth, K. and Hov, Ø. (eds.): The EMEP monitoring strategy 2004-2009. Background document with
1110 justification and specification of the EMEP monitoring programme 2004-2009, Kjeller, NILU
1111 (EMEP/CCC, 09/2003), 2003.
- 1112
- 1113 Tørseth, K., Semb, A., Schaug, J., Hanssen, J. E., and Aamlid, D.: Processes affecting deposition of
1114 oxidised nitrogen and associated species in the coastal areas of Norway, *Atm. Environ.*, 34, 2, 207-217,
1115 2000.
- 1116
- 1117 Tørseth, K., Aas, W., Breivik, K., Fjæraa, A. M., Fiebig, M., Hjellbrekke, A. G., Lund Myhre, C.,
1118 Solberg, S., and Yttri, K. E.: Introduction to the European Monitoring and Evaluation Programme
1119 (EMEP) and observed atmospheric composition change during 1972–2009, *Atmos. Chem. Phys.*, 12,
1120 5447–5481 www.atmos-chem-phys.net/12/5447/2012/doi:10.5194/acp-12-5447-2012, 2012.
- 1121
- 1122 UNECE: 1999 Protocol to Abate Acidification, Eutrophication and Ground-level Ozone to the
1123 Convention on Long-range Transboundary Air Pollution, as amended on 4 May 2012, Geneva:
1124 UNECE, 2013.
- 1125
- 1126 UNECE: Monitoring strategy for the Cooperative Programme for Monitoring and Evaluation of the
1127 Long-range Transmission of Air Pollutants in Europe for the period 2020–2022, UNECE, Geneva,
1128 Decision 2019/1, ECE/EB.AIR/144/Add.1, 2019
- 1129
- 1130 Viana, M., Kuhlbusch, T. A. J., Querol, X., Alastuey, A., Harrison, R. M., Hopke, P. K., Winiwarter,
1131 W., Vallius, M., Szidat, S., Prévôt, A. S. H., Hueglin, C., Bloemen, H., Wählin, P., Vecchi, R., Miranda,
1132 A. I., Kasper-Giebl, A., Maenhaut, W., and Hitzenberger, R.: Source apportionment of particulate matter
1133 in Europe: A review of methods and results, *J. Aerosol Sci.*, 39, 827–849,
1134 doi:10.1016/j.jaerosci.2008.05.007, 2008.
- 1135
- 1136 Waked, A., Favez, O., Alleman, L. Y., Piot, C., Petit, J.-E., Delaunay, T., Verlinden, E., Golly, B.,
1137 Besombes, J.-L., Jaffrezo, J.-L., and Leoz-Garziandia, E.: Source apportionment of PM₁₀ in a north-
1138 western Europe regional urban background site (Lens, France) using positive matrix factorization and
1139 including primary biogenic emissions, *Atmos. Chem. Phys.*, 14, 3325–3346,
1140 <https://doi.org/10.5194/acp-14-3325-2014>, 2014.
- 1141
- 1142 Weber, S., Salameh, D., Albinet, A., Alleman, L. Y., Waked, A., Besombes, J.-L., Jacob, V., Guillaud,
1143 G., Meshbah, B., Rocq, B., Hulin, A., Dominik-Sègue, M., Chrétien, E., Jaffrezo, J.-L., and Favez, O.:
1144 Comparison of PM₁₀ Sources profiles at 15 French sites using a harmonized constrained positive matrix



- 1145 factorization approach, *Atmosphere*, 10, 310, <https://doi.org/10.3390/atmos10060310>, 2019.
- 1146
- 1147 WHO: Review of evidence on health aspects of air pollution – REVIHAAP Project, Technical Report,
1148 Copenhagen: WHO Regional Office for Europe, 2013.
- 1149
- 1150 Winiwarter, W., Haberl, H., and Simpson, D.: On the boundary between man-made and natural
1151 emissions: Problems in defining European ecosystems, *J. Geophys. Res.*, 104, 8153–8159, 1999.
- 1152
- 1153 Yttri, K. E., Aas, W., Bjerke, A., Cape, J. N., Cavalli, F., Ceburnis, D., Dye, C., Emblico, L., Facchini,
1154 M. C., Forster, C., Hanssen, J. E., Hansson, H. C., Jennings, S. G., Maenhaut, W., Putaud, J. P., and
1155 Tørseth, K.: Elemental and organic carbon in PM₁₀: a one year measurement campaign within the
1156 European Monitoring and Evaluation Programme EMEP, *Atmos. Chem. Phys.*, 7, 5711–5725,
1157 <https://doi.org/10.5194/acp-7-5711-2007>, 2007a.
- 1158
- 1159 Yttri, K. E., Dye, C., and Kiss, G.: Ambient aerosol concentrations of sugars and sugar-alcohols at four
1160 different sites in Norway, *Atmos. Chem. Phys.*, 7, 4267–4279, [https://doi.org/10.5194/acp-7-4267-](https://doi.org/10.5194/acp-7-4267-2007)
1161 [2007](https://doi.org/10.5194/acp-7-4267-2007), 2007b.
- 1162
- 1163 Yttri, K. E., Simpson, D., Stenstrom, K., Puxbaum, H., and Svendby, T.: Source apportionment of the
1164 carbonaceous aerosol in Norway - quantitative estimates based on C-14, thermal-optical and organic
1165 tracer analysis, *Atmos. Chem. Phys.* 11, 9375–9394, 2011a.
- 1166
- 1167 Yttri, K. E., Simpson, D., Nojgaard, J. K., Kristensen, K., Genberg, J., Stenstrom, K., Swietlicki, E.,
1168 Hillamo, R., Aurela, M., Bauer, H., Offenberg, J. H., Jaoui, M., Dye, C., Eckhardt, S., Burkhardt, J. F.,
1169 Stohl, A., and Glasius, M.: Source apportionment of the summer time carbonaceous aerosol at Nordic
1170 rural background sites, *Atmos. Chem. Phys.* 11, 13339–13357, 2011b.
- 1171
- 1172 Yttri, K. E., Lund Myhre, C., Eckhardt, S., Fiebig, M., Dye, C., Hirdman, D., Ström, J., Klimont, Z. and
1173 Stohl, A.: Quantifying black carbon from biomass burning by means of levoglucosan – a one year time
1174 series at the Arctic observatory Zeppelin, *Atmos. Chem. Phys.*, 14, 6427–6442, 2014. doi:10.5194/acp-
1175 [14-6427-2014](https://doi.org/10.5194/acp-14-6427-2014), 2014.
- 1176
- 1177 Yttri, K. E., Simpson, D., Bergström, R., Kiss, G., Szidat, S., Ceburnis, D., Eckhardt, S., Hueglin, C.,
1178 Nøjgaard, J. K., Perrino, C., Pizzo, I., Prevot, A. S. H., Putaud, J.-P., Spindler, G., Vana, M., Zhang, Y.-
1179 L., and Aas, W.: The EMEP Intensive Measurement Period campaign, 2008–2009: characterizing
1180 carbonaceous aerosol at nine rural sites in Europe, *Atmos. Chem. Phys.*, 19, 4211–4233, 2019.
1181 <https://doi.org/10.5194/acp-19-4211-2019>.



1182

1183 Zotter, P., Ciobanu, V. G., Zhang, Y. L., El-Haddad, I., Macchia, M., Daellenbach, K. R., Salazar, G.
1184 A., Huang, R.-J., Wacker, L., Hueglin, C., Piazzalunga, A., Fermo, P., Schwikowski, M., Baltensperger,
1185 U., Szidat, S., and Prévôt, A.S.H.: Radiocarbon analysis of elemental and organic carbon in Switzerland
1186 during winter-smog episodes from 2008 to 2012 – part 1: source apportionment and spatial variability,
1187 Atmos. Chem. Phys. Discuss., 14, pp. 15591-15643, 2014.

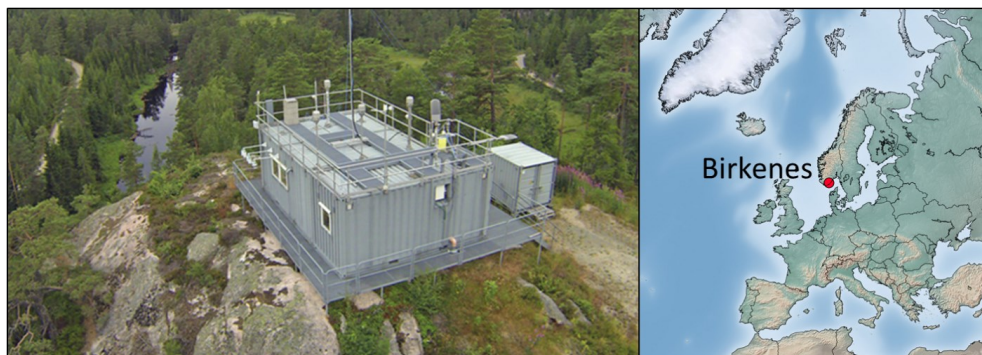
1188

1189 Zotter, P., Herich, H., Gysel, M., El-Haddad, I., Zhang, Y., Mocnik, G., Hüglin, C., Baltensperger, U.,
1190 Szidat, S., and Prévôt, A. S. H.: Evaluation of the absorption Ångström exponents for traffic and wood
1191 burning in the Aethalometer-based source apportionment using radiocarbon measurements of ambient
1192 aerosol, Atmos. Chem. Phys., 17, 4229–4249, [www.atmos-chem-](http://www.atmos-chem-phys.net/17/4229/2017/doi:10.5194/acp-17-4229-2017)
1193 [phys.net/17/4229/2017/doi:10.5194/acp-17-4229-2017](http://www.atmos-chem-phys.net/17/4229/2017/doi:10.5194/acp-17-4229-2017), 2017.

1194



1195 **Figures**



1196

1197 **Figure 1: The Birkenes Observatory (58°23' N, 8°15' E; 219 m asl) lies in the Boreo-nemoral zone, 20 km from the**
1198 **Skagerrak coastline in Southern Norway.**

1199

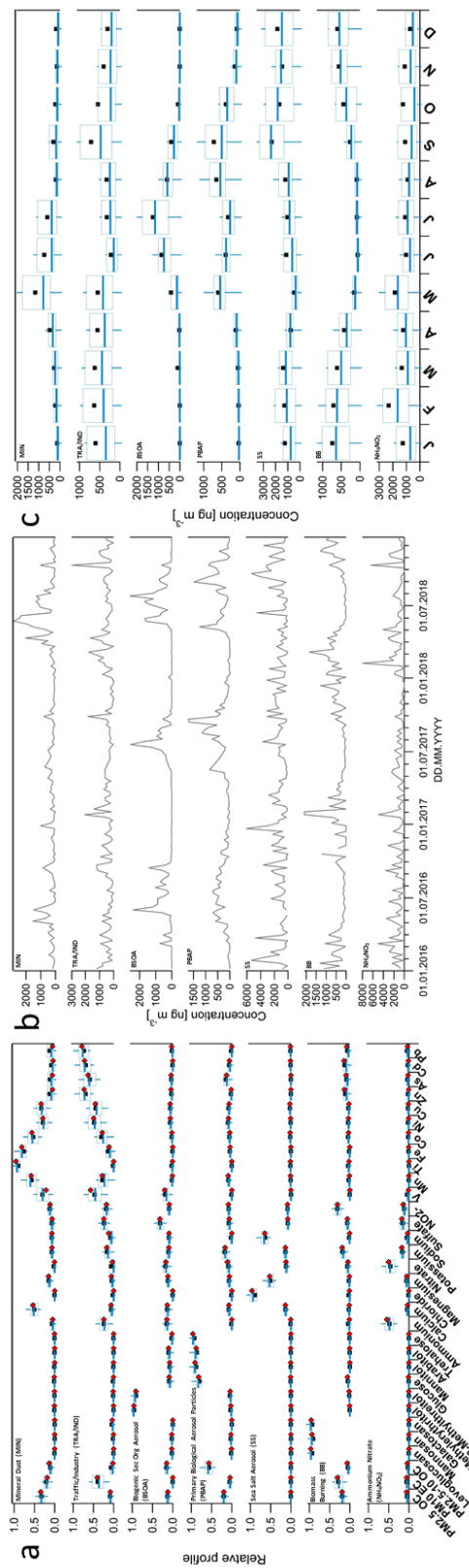
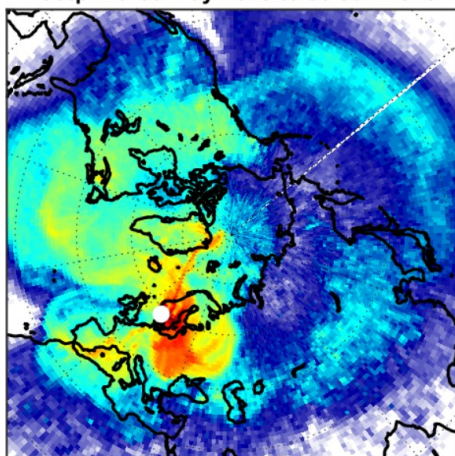


Figure 2: Results from PMF for Birkenes 2016–2018. a) Factor profiles b) Factor time series c) aggregated monthly data. Boxes in a), c) show statistics from bootstrapped solutions (n=5000): percentiles 25/75 (box), median (horizontal line) and 10/90 (whiskers). Black markers in a) and 10/90 (whiskers). Red markers in a) show the base factor profiles.



Footprint: 30-May-2018 to 06-Jun-2018



0.00 0.00 0.02 0.06 0.25 1.00 4.00 16.00

Averaged emission sensitivity [ns m^{-2}]

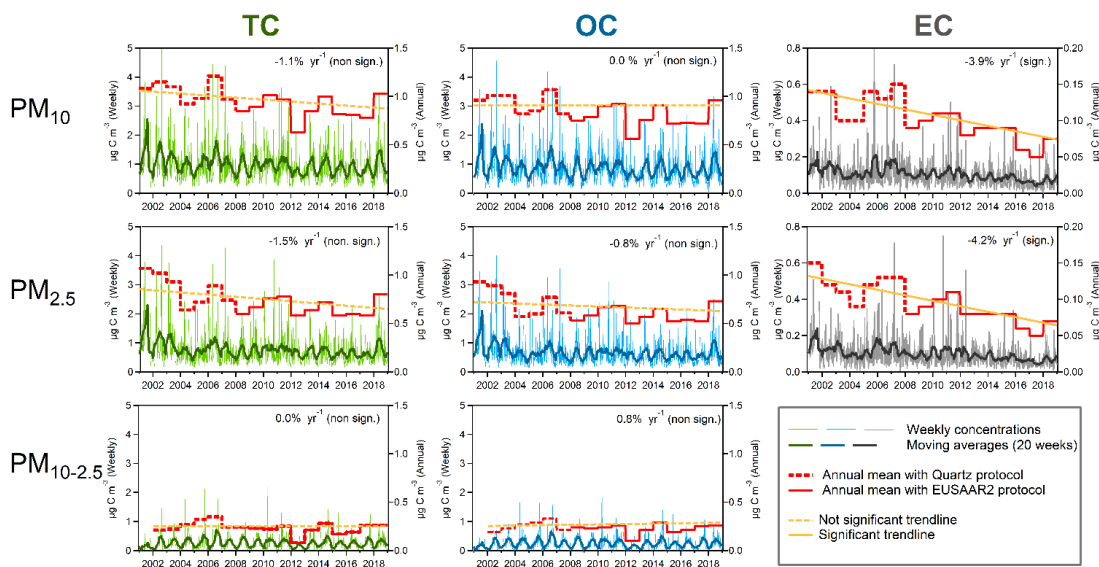
1204

1205

1206

Figure 3: Footprint emission sensitivities calculated using the FLEXPART model for the period 30 May–6 June 2018 at the Birkenes Observatory.

1207



1208

1209

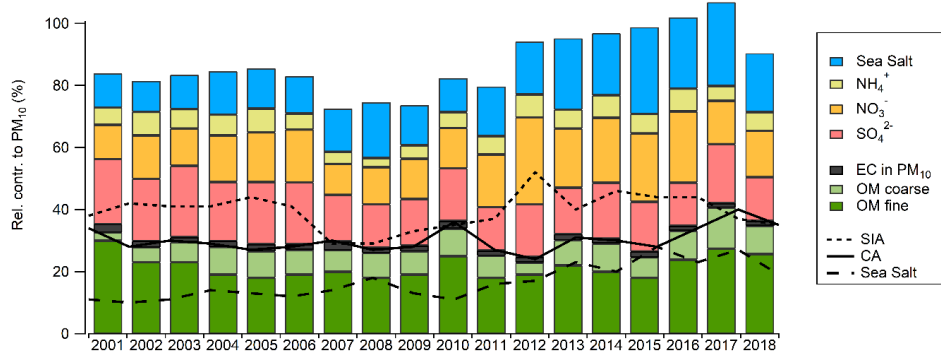
1210 **Figure 4: Ambient aerosol concentrations of TC, OC and EC in PM₁₀ (Upper panels), in PM_{2.5} (Mid-Panels), and TC**

1211

and OC in PM_{10-2.5} (Lower panels), presented as weekly (168 h) and annual mean concentrations for the Birkenes

1212

Observatory for 2001–2018. The trendlines account for the protocol shift.



1213

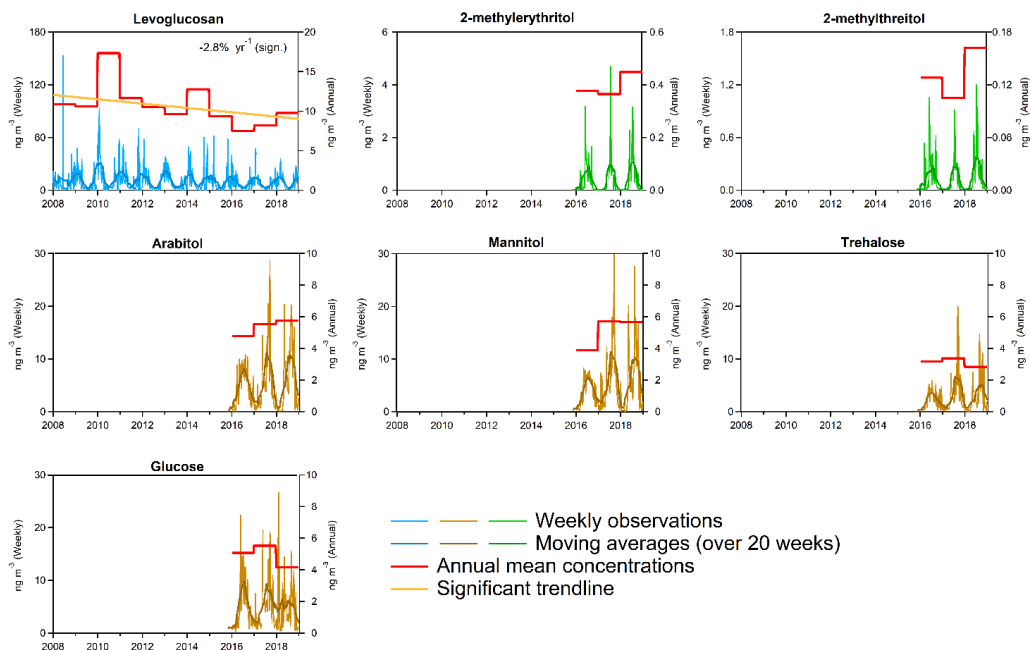
1214

1215

1216

Figure 5: Mass closure of PM₁₀ for Birkenes for the period 2001–2018 (Unit: %). Notation: Sea salt = Sum of Na⁺, Mg²⁺, Cl⁻; SIA = Secondary inorganic aerosol (SIA) = Sum of SO₄²⁻, NO₃⁻, NH₄⁺; CA = Carbonaceous aerosol; OM = Organic matter. OM is calculated using OC:OM=1.9 (Yttri et al., 2011a).

1217



1218

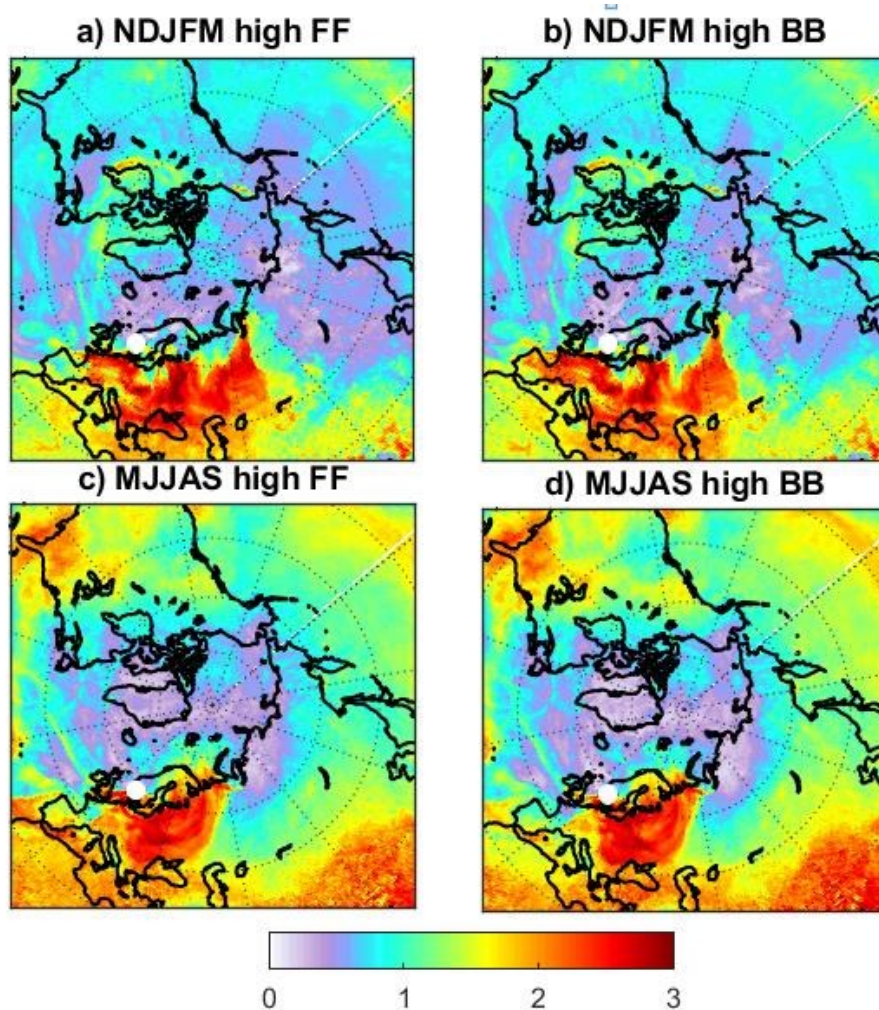
1219

1220

1221

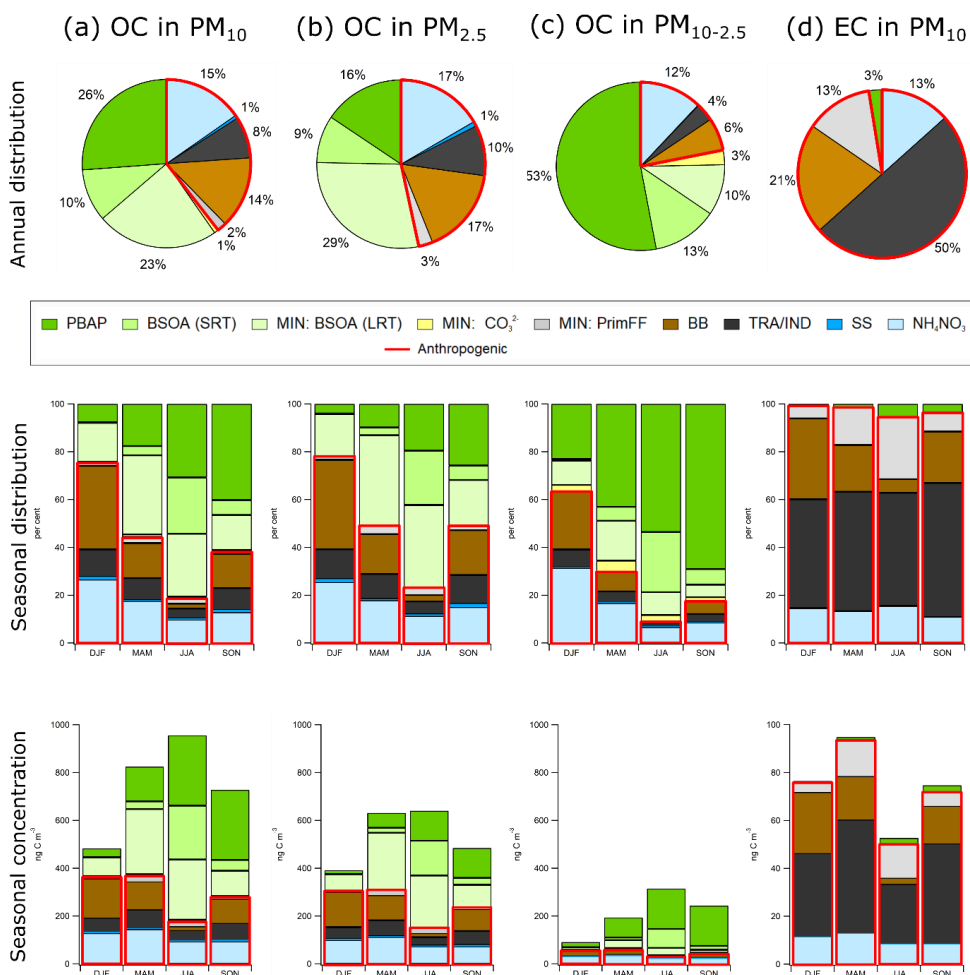
Figure 6: Ambient aerosol concentrations of organic tracers in PM_{10} . Levoglucosan, 2-methylerythritol and 2-methylthreitol (Upper panels), arabitol, mannitol, trehalose (Mid-Panels), and glucose (Lower panel), presented as weekly (168 h) and annual mean concentrations for the Birkenes Observatory for the period 2008–2018.

1222



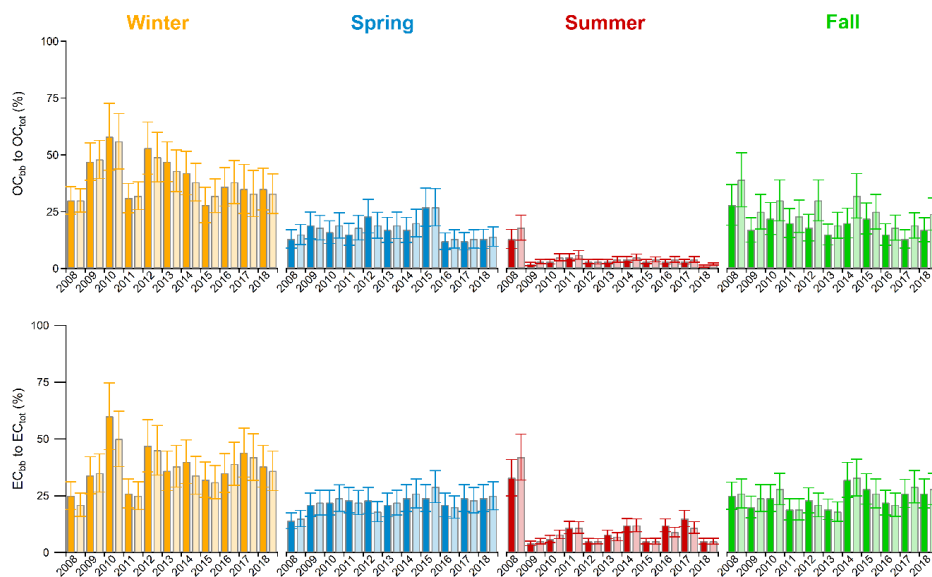
1223
1224 **Figure 7:** 70th percentiles of eBC_{ff} (left panels, a and c) and eBC_{bb} (right panels, b and d) for winter (NDJFM) and
1225 summer (MJJAS). The color-coding shows the ratio of residence times for footprint sensitivities during measurements
1226 exceeding the 70th percentile and the average footprint sensitivity.

1227



1228
 1229 **Figure 8:** Factor contributions to OC in PM₁₀ (a), PM_{2.5} (b), PM_{10-2.5} (c), and EC in PM₁₀ (d) at Birkenes (2016–2018)
 1230 (upper panels), and divided into seasons (middle and lower panels), as determined by positive matrix factorisation. The
 1231 factors enclosed by the full red line represents anthropogenic sources. The OC content of the MIN factor is divided into
 1232 long range transported BSOA (OC_{BSOA,LRT}) and primary OC from fossil fuel combustion (OC_{PrimFF}) following Eq. (1),
 1233 and carbonate carbon (OC_{CO32-}) (Sect. 2.4.1).

1234



1235
1236 **Figure 9: Relative contribution of OC_{bb} to OC_{tot} (upper panel) and EC_{bb} to EC_{tot} (lower panel) in PM_{10} (dark colors)**
1237 **and in $PM_{2.5}$ (light colors), as a function of season at Birkenes for 2008–2018 (DJF = Winter; MAM = Spring; JJA =**
1238 **Summer; SON = Fall).**

1239



1240

1241 **Tables**

1242 **Table 1: Variables describing the biomass burning source derived from the PMF BB factor in the present study, and**
1243 **comparable variables obtained by ^{14}C -analysis reported by Zotter et al. (2014).**

Present study	Zotter et al. (2014) ¹
OC/Levoglucosan (in PM_{10}) = 12.7	$\text{OC}_{\text{NF}}/\text{Levoglucosan}$ (in PM_{10}) = 12.6 ± 3.1
OC/Levoglucosan (in $\text{PM}_{2.5}$) = 11.1	
EC/Levoglucosan (in PM_{10}) = 1.96	$\text{EC}_{\text{NF}}/\text{Levoglucosan}$ (in PM_{10}) = 1.72 ± 0.59
OC/EC (in PM_{10}) = 6.5	$\text{OC}_{\text{NF}}/\text{EC}_{\text{NF}}$ (in PM_{10}) = 7.7 ± 2.1
OC/EC (in $\text{PM}_{2.5}$) = 5.7	

1244 ¹North of the Alps

1245 Notation: OC_{NF} = Non-fossil OC; EC_{NF} = Non-fossil EC

1246

1247



1248 **Table 2: Biomass burning fraction derived from the PMF and the aethalometer model. Aethalometer model 1 shows**
1249 **the biomass burning fraction obtained by the default pair of Absorption Ångström Exponents (AAE) suggested by**
1250 **Zotter et al. (2014), whereas Aethalometer model 2 show the biomass burning fraction obtained using the pair of AAEs**
1251 **derived from PMF.**

	PMF	Aethalometer model 1	Aethalometer model 2
Biomass burning fraction	0.27	0.48	0.28
Fossil AAE	0.93	0.9 (Zotter et al. 2017)	0.93 (from PMF)
Biomass burning AAE	2.04	1.68 (Zotter et al. 2017)	2.04 (from PMF)

1252



Table 3: OC_{BSOA} , short-range transported (SRT) and long-range transported (LRT), and OC_{PBAP} concentrations and their relative contribution to OC in PM_{10} at Birkenes in August, as obtained by Latin Hypercube Sampling (Yttri et al., 2011b) and by PMF (present study).

	Reference	Approach	$OC_{\text{BSOA,SRT}}$ ($\mu\text{g C m}^{-3}$)	$OC_{\text{BSOA,SRT}}/OC$	$OC_{\text{BSOA,SRT+LRT}}$ ($\mu\text{g C m}^{-3}$)	$OC_{\text{BSOA,SRT+LRT}}/OC$	OC_{PBAP} ($\mu\text{g C m}^{-3}$)	OC_{PBAP}/OC
August 2009	Yttri et al. (2011b)	LHS ¹			505^{a} ($408-598$) ^{2,3}	0.48^{a} ($0.38-0.58$) ^{2,3}	290^{b} ($213-380$) ²	0.31^{b} ($0.22-0.40$) ²
August 2016	Present study	PMF	115	0.19	173	0.28	318	0.52
August 2017	Present study	PMF	183	0.19	252	0.26	553	0.57
August 2018	Present study	PMF	159	0.20	316	0.40	287	0.36
August 2016–2018	Present study	PMF	152	0.19	247	0.31	386	0.48

1. 50th percentile
2. 10th–90th percentile
3. LHS-approach includes both $OC_{\text{BSOA,SRT}}$ and $OC_{\text{BSOA,LRT}}$

1253
 1254

1255
 1256
 1257
 1258